Lawrence Berkeley National Laboratory
Recent Work

Title
REACTION PROFILES IN POROUS ELECTRODES

Permalink
https://escholarship.org/uc/item/12z3k0vp

Authors
Katan, T.
Carlen, P.J.

Publication Date
1985-05-01

eScholarship.org Powered by the California Digital Library
University of California

LBL-19727
UC-94c

Lawrence Berkeley Laboratory
UNIVERSITY OF CALIFORNIA

RECEIVED
LAWRENCE
OCT 18 1985
LIBRARY AND
DOCUMENTS SECTION

APPLIED SCIENCE DIVISION

REACTION PROFILES IN POROUS ELECTRODES
Final Report

T. Katan and P.J. Carlen

May 1985

TWO-WEEK LOAN COPY
This is a Library Circulating Copy
which may be borrowed for two weeks.

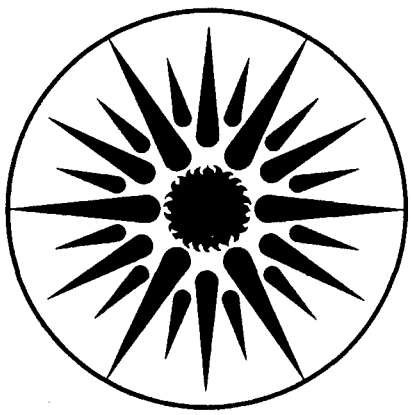

APPLIED SCIENCE DIVISION

Prepared for the U.S. Department of Energy under Contract DE-AC03-76SF00098

LBL-19727

DISCLAIMER

This document was prepared as an account of work sponsored by the United States Government. While this document is believed to contain correct information, neither the United States Government nor any agency thereof, nor the Regents of the University of California, nor any of their employees, makes any warranty, express or implied, or assumes any legal responsibility for the accuracy, completeness, or usefulness of any information, apparatus, product, or process disclosed, or represents that its use would not infringe privately owned rights. Reference herein to any specific commercial product, process, or service by its trade name, trademark, manufacturer, or otherwise, does not necessarily constitute or imply its endorsement, recommendation, or favoring by the United States Government or any agency thereof, or the Regents of the University of California. The views and opinions of authors expressed herein do not necessarily state or reflect those of the United States Government or any agency thereof or the Regents of the University of California.

LBL-19727

REACTION PROFILES IN POROUS ELECTRODES

Final Report

May 1985

by

Theodore Katan and P.J. Carlen

Lockheed Palo Alto Research Laboratory
Lockheed Missiles & Space Company, Inc.
3251 Hanover Street
Palo Alto, California 94304

for

Technology Base Research Project
Lawrence Berkeley Laboratory
University of California
Berkeley, California 94720

This work was supported by the Assistant Secretary for Conservation and Renewable Energy, Office of Energy Systems Research, Energy Storage Division of the U.S. Department of Energy under Contract No. DE-AC03-76SF00098, Subcontract No. 4517310 with the Lawrence Berkeley Laboratory.

NOTICE

This report was prepared as an account of work sponsored by an agency of the United State Government. Neither the United States Government nor any agency thereof, nor any of their employees, makes any warranty, expressed or implied, or assumes any legal liability or responsibility for any third party's use of the results of such use of any information, apparatus, product, or process disclosed in this report or represents that its use by such third party would not infringe privately owned rights.

FOREWORD

This report describes an experimental program designed to develop the secondary alkaline zinc electrode in high-performance aqueous batteries for electric vehicle applications. It describes experiments which, for the most part, are a continuation of those reported in Basic Studies on Nickel-Zinc Batteries, LMSC-D681417, Final Report, Contract EM-78-C-01-5165, 28 November 1979, and in Basic Studies on Nickel-Zinc Batteries, LMSC-D811282, Final Report, Contract S/C 4503610, 30 August 1981.

ABSTRACT

An experimental program was conducted to ascertain causes of alkaline zinc electrode shape change and to determine the development of reaction profiles within the pores of porous zinc electrodes. Various analog electrochemical cells were operated to isolate and evaluate the individual processes occurring during charge and discharge.

It was found that both edge effects and osmosis can be responsible for the shape change phenomenon. Edge effects could penetrate up to 1.5 mm into the electrode at a frontal current density of 200 $mAcm^{-2}$ while making the edge 20 mV more negative during discharge, causing a corrosion current of about 0.4 $mAcm^{-2}$. Also during discharge, the increase in zincate-ion concentration at the zinc electrode can cause osmotic flow through a cellophane separator towards the zinc at rates higher than $1.5 \times 10^{-4} cm^3 cm^{-2} sec^{-1}$. Both of these processes are sufficient in themselves, individually, to cause shape change during cycling at moderate current densities, 20 to 100 $mAcm^{-2}$.

Electroosmosis was found to be at least one order of magnitude less than the osmosis that can be developed and is considered as negligible.

Penetration depths of the reaction profile were found to be essentially constant, indicating that a typical zinc electrode should be no more than 0.02 cm thick. The reaction profiles at various current densities showed very little polarization, less than 60 mV, until current densities in excess of 500 $mAcm^{-2}$ were applied and the IR drop within the electrode became comparable to and governed the overall polarization.

Penetration depths at the edges, measured lateral to the overall current, became greater with increasing current density once a critical current density was exceeded.

The shape change phenomenon was essentially stopped by roughening the edges of the zinc electrode's substrate to decrease the local current density at the edges of a planar electrode. Also effective was the use of a counter electrode a few millimeters smaller than the zinc negative. In these tests of over 1000 cycles, only a polypropylene screen separator was used with a silver-oxide counter electrode.

ACKNOWLEDGMENTS

This work was performed by Dr. T. Katan and Ms. P. J. Carlen in the Chemistry Laboratory of the Lockheed Palo Alto Research Laboratories (LPARL), Dr. F. G. Borgardt, Manager. The authors wish to acknowledge the assistance of the LPARL Metallurgy Laboratory, particularly of Mr. A. R. Hansen for the preparation and polishing of the single-pore substrates. We thank Drs. F. McLarnon and K. Kinoshita of the Lawrence Berkeley Laboratory for their program direction and support. We also sincerely appreciate the many suggestions and remarks of our colleagues and Dr. A. R. Landgrebe, Department of Energy, Washington, D.C.

TABLE OF CONTENTS

LIST OF ILLUSTRATIONS

Section 1
INTRODUCTION

1.1 BACKGROUND AND SCOPE OF REPORT

In this work, analog single-pore cells and other specially designed cells are used to examine reactions that occur in porous zinc electrodes. Experiments are designed to help bring an understanding of the processes occurring at secondary alkaline zinc electrodes and impact nickel-zinc, zinc/air, etc., battery technologies and, thereby, to help in the development of these batteries.

This report describes the technical results obtained at the Lockheed Palo Alto Research Laboratory (LPARL) for The Division of Energy Storage Systems of The Department of Energy (DOE). The work was monitored by the Lawrence Berkeley Laboratory under S/C 4517310, Reaction Profiles In Porous Electrodes, and it is a continuation of two previous DOE contracts, EM-78-C-01-5165 (Ref. 1) and S/C 4503610 (Ref. 2).

Much of the technical background for this work is given in the original report for the first DOE contract (Ref. 1). Here, we briefly describe technical background and approach, to the extent needed to preserve continuity.

1.2 PROBLEM AREAS OF THE NICKEL-ZINC BATTERY

The advantages of the nickel-zinc battery for electric vehicle applications have been variously described in the literature (Refs. 3, 4). Yao and Birk (Ref. 5) in their review of advanced secondary batteries and Landgrebe et al. (Ref. 3) discuss the advanced state of development of the nickel positive. Nickel positives reportedly yield 1,000 deep cycles in the nickel-hydrogen system (Ref. 5). However, certain problems remain with the zinc electrode.

Difficulties of the alkaline zinc negative are formidable and have been described by Lander (Ref. 6) and by Falk and Salkind (Ref. 7). Cycle life of the nickel-zinc cell is limited by the zinc electrode (Ref. 7) to 200 to 300 cycles. The principal failure modes are as follows (Ref. 6):

- Shape change of the zinc electrode after cycling;
- Drying of the zinc negative after deep discharge;
- Shorting by zinc dendrite growth at high local overpotentials;
- Loss of active zinc area when large zinc crystals form after prolonged cycling.

For small depths of discharge and charge and with the use of cellophane membranes, the principal difficulty is zinc-electrode shape change or zinc displacement during cycling. The displacement is not caused by gravitational forces and can occur in various directions, for instance, upwards or from the electrode center towards the edges (Ref. 8), although it is usually towards the center. As a result, some parts of the electrode are depleted in zinc while other parts become thicker. Deterioration in performance soon follows.

The problem has been extensively studied (Refs. 6, 8), but there are still no reliable methods for dealing with it. It has been reported that the development of a long-lived, reversible zinc electrode "remains one of the major tasks in the work on cells with aqueous electrolytes" (Ref. 8).

It is the objective of this program to conduct more-basic studies that result in a set of recommendations and guidelines for zinc-electrode manufacture of static-electrolyte nickel/zinc cells. These recommendations and guidelines will be hopefully tested in the future by cycling of actual cells, for example, at the Lawrence Berkeley Laboratory's cell-cycling facility or at the laboratories of battery manufacturers.

1.3 EXPERIMENTAL APPROACH

The complexities of the processes occurring at porous zinc electrodes during cycling are evident from considerations of the multitudinous steps involved during cycling. Cathodic reaction is commonly the reduction of a saturated zincate-ion solution containing sparingly-soluble, solid zinc oxide. A conductive grid, usually copper or silver, is used to channel electron flow to sites of reduction which are either on the grid itself or on the deposited porous zinc. Anodic steps include the formation of supersaturated zincate-ion solution and zinc oxide or hydroxide precipitates.

A typical zinc electrode for a practical cell therefore consists of a network of conductive material with active zinc reactant and zinc oxide and hydroxide product distributed throughout the conductive network that maintains electron flow and reaction area. Some degree of porosity is required so that electrolyte may contact the reactant in depth to make a large reaction area available. A balance is formed between electronic, mass, and ionic fluxes determined largely by the electrode's morphology which in turn evolves during cycling according to local conditions.

It is evident that a simplified system is needed to study these numerous processes that take place in the zinc electrode. As reported earlier (Refs. 1 and 2) an analog single-pore cell is constructed in our work to isolate performance along a single pore. In this way the electrode system is simplified enough to allow study of the various complicated steps.

The elctrode system consists of two zinc slugs, 1 x 0.6 x 0.3 cm, 0.3 cm apart, embedded in the end of an epoxy, cylindrical metallurgical mount, and polished flat on a metallurgical wheel to a submicron finish. A 20-micron thick Teflon spacer is placed around the zinc electrodes, and an epoxy cover slide containing multiple reference electrodes is placed over the zinc electrodes and added electrolyte. This well-characterized geometrical configuration and arrangement can be used to examine potential and concentration gradients that form under a variety of conditions, and performance can be related to other, more complex electrode morphologies once this simplified electrode is understood.

Additionally, in this work, a planar, 1 x 1 cm sliver electrode is used to examine the influence of separator materials and edge effects on shape change. A polished silver electrode is plated with a thin layer of zinc, and the movement of the zinc is observed as this electrode is cycled in the presence of cellophane or other separator material.

Planar electrodes with small amounts of zinc can be charged and discharged to considerable depths within a few seconds so that several thousand cycles can be obtained in one day. Usually, an actual zinc electrode requires several hours for a cycle, and several months may be required to obtain 1000 cycles.

Section 2
MULTIPLE-REFERENCE ZINC ELECTRODE

2.1 INTRODUCTION

Despite considerable efforts in the past, workers have not been able to measure potential profiles within the confines of commercial zinc electrodes where pores are small, on the order of 20 microns or less in effective diameter. Such measurements are not possible, in situ, because of the pores' inaccessibility and miniscule dimensions.

As a result, little is known of the dominant processes that occur, of their location along the pores, and of their relation to electrode structure. Porous zinc electrodes have accordingly not often been optimally utilized, nor have their structures been clearly designated.

It is apparent, however, that a better knowledge of processes and reactions within the pores, together with their relation to structure, materially helps in guiding electrode design and manufacture. To gain this knowledge, small electrochemical systems were studied that simulate and resemble the pores of real electrodes. By use of a pore analog, in-situ viewing and potential/position measurements were effected while a well-characterized geometry was maintained. Studies of behavior of electrochemical analogs can provide insight on the performance of real porous electrodes and enable detection of processes that cannot be observed in commercially prepared electrodes or anticipated by a-priori mathematical modeling (Ref. 9). Useful physicochemical parameters can be extracted to assist manufacture.

In the study reported in this section, we employ a single-pore electrochemical cell that is an analog of a pore in a porous zinc electrode in KOH electrolyte. We describe the evolution of potential profiles within the pore during discharge and relate

this with the precipitation and movement previously reported of ZnO into the pore (Ref. 2). The perturbation and relaxation of the OH^- concentration profile in the pore are also determined during a given discharge and after its subsequent termination. Fluctuations in (OH^-) are examined for their correspondence to ZnO precipitation and to Zn dissolution, reactions that release and consume OH^-, respectively.

Here, we also examine potential profiles in an attempt to determine the significance of edge effects that may cause shape change during cycling.

The measurement of potential distribution within a pore as reported here has not been a very common experimental procedure. Thus, while several workers have sectioned electrochemical analogs of electrode pores, post mortem, to obtain reaction profiles (Refs. 10-15) or measured current distributions with analogs that were initially segmented into isolated sections (Refs. 16-21), only Brodd in 1966 (Ref. 22) appears to have examined potential profiles in a simulated pore, aside from an effort parallel to ours carried out at the Lawrence Berkeley Laboratory (Ref. 23).

The work on potential profiles in pores is limited probably because potentials of reference electrodes may change when concentrations vary within small, reacting pores. In the work reported here, we take advantage of the dependence of the potential of the zinc electrode on (OH^-) indicated by Bode et al (Ref. 24) and obtain an approximate (OH^-) distribution. Measurement of potential profiles thus has an advantage of yielding information on concentration distributions that is not directly obtainable by measurements of current distribution.

Experimentally, the basic technique applied in this work is to intermittently place the discharging pore on open circuit for a few seconds. The potential difference between the reference and working electrodes at open and closed circuit yields the potential or polarization distribution. The open-circuit potentials are used to calculate or estimate the OH^- concentration profile, provided concentrations at the reference electrodes remain relatively unchanged and liquid junction potentials are negligible. Both zinc and Ag/Ag_2O reference electrodes were used in the course of this work.

As a check for possible drift in potential of the actual multiple-reference array of electrodes, in some experiments a separate Hg/HgO reference electrode was placed at some distance from the multiple-reference array (2 cm). The concentration at the Hg/HgO reference electrode could not change, and it is relatively insensitive to OH^- concentration changes. Thus, a stable reference could be established to determine the extent of drift of each reference. Also, within the reference array, one electrode is placed far in the rear, over 1 cm away, and it can also be used as a stable basic reference to check the other references.

2.2 EXPERIMENTAL

The single-pore cell assembly in this study was essentially described in a previous publication (Ref. 25; see also Ref. 2), however, with one notable exception. In the present study, the transparent Lucite cover slide on the cell is replaced by an epoxy cover slide containing ten zinc reference electrodes, Figure 1.

The Lucite cover slide in the prior study allowed visual examinations and measurements of ZnO precipitate penetration rates. In this work, we maintain the same internal geometry of the pore and apply the same galvanostatic currents, but now measure potential along the zinc pore.

The 20-micron spacing is fixed by a Teflon-film spacer, Figure 1, between the two flat surfaces of the epoxy mounts that are metallurgically polished to a submicron finish with diamond abrasive powder, washed with distilled water, and dried in a room-temperature air stream before the experiment. This 20-micron spacing is accurate to within $\pm$5 percent, as determined by a microscopic measuring technique and checked by conductivity measurements.

Both the upper and lower epoxy mounts, Figure 2, are cylindrical in shape, 2.54 cm in diameter. The lower mount contains two matching zinc electrodes, having 1 x 0.7 cm of exposed rectangular area, 0.3 cm apart along the length, in the flat surface plane, and two screws threaded from the bottom for connecting external electrical current from a galvanostat. Current is passed through the electrolyte in the space between the electrodes. The distance from the edge of the electrode inward is designated as the penetration depth of the pore which is defined by the electrolyte, 0.0020 x 1.00 cm in cross section from electrode to electrode and along the longitudinal direction of the pore.

The upper epoxy mount contains in its center ten threads of either zinc or silver metal connected to an electrical switch above and leading to the flat surface below. The threads are 0.0004 x 0.008 cm in cross section, they are all in a plane, exposed and positioned with respect to the working electrode as shown in Figure 3. The threads are previously vapor deposited on an alumina plate, using microelectronic methods, before being embedded in the upper mount. A ten-position switch is used to connect each reference electrode versus the working electrode while the others are isolated.

During an experiment, we used an EG&G PARC Model 175 Universal programmer, an EG&G PARC Model 173 Potentiostat/Galvanostat, a Soltec Model VP-64325 XY recorder, a Soltec Model 1241 Strip-chart recorder, and a Systron Donner Model 7004A Digital Multimeter, to apply constant current to the electrodes at preselected time intervals and to monitor the various potential differences.

In one set of experiments, during discharge, the closed circuit potentials of the multiple-reference arrays were continually measured by sweeping the switch, taking about 10 to 15 seconds per sweep. Periodically, the applied current was interrupted, and the open-circuit potentials were obtained with one sweep before reapplying the current. In another set of experiments, the open-circuit potentials of the multiple array were measured periodically during cycling versus the working electrode, and then immediately afterward the open-circuit potentials of the multiple array were measured versus the Hg/HgO reference electrode placed at the outside edge of the epoxy cylinders.

In some experiments the multiple-reference electrode array was placed so that potentials could be measured from the front edge of the zinc electrode inwards towards the back of the zinc electrode. In other experiments the potentials were measured along the front edge of the zinc electrode, from the corner inwards towards the center of the front edge.

Before an experiment, a drop of electrolyte was placed on the lower mount with its spacer in place, the upper mount was placed on the drop and positioned with a microscope focused through the transparent mount onto the threads and working electrode. Constant current was then applied while the switch was swept to record the potentials of the reference electrodes. Room temperature was 22.3 $\pm$1.0°C.

When the silver reference electrode array was used, the silver electrodes were first individually charged to the Ag_2O/Ag potential by applying 0.2 microamp anodically until the AgO/Ag_2O peak potential was approached.

The electrolyte was prepared from 10-M KOH that was in contact with finely divided ZnO for a period of 4 months before the experiment, all ACS reagent grade. Analyses of the solid-free electrolyte after the 4 months indicated that the electrolyte was then 7.72 M OH^- and 1.14 M $Zn(OH)_4^=$, with an acuracy of ± 5 percent.

2.3 RESULTS AND DISCUSSION

2.3.1 Primary Potential Distribution

The potential profiles during the first 10-15 seconds required for a potential sweep are shown in Figures 4 and 5. In these figures, polarizations are plotted versus the distance of penetration into the zinc pore. Open-circuit potentials were initially at -1.261 volt vs. SHE, and we see from Figures 4 and 5 that the closed circuit potentials at the front edge varied from 0.050 to 0.70 volt in a more positive direction, depending on the applied current. The larger the current, the greater is the polarization.

2.3.1.1 Penetration Depth

As may be anticipated there is an "exponential-appearing" decrease in the polarization for increasing penetration distance into the pore (Ref. 26). Also, examination of the developed family of curves reveals that the polarization commences to "level out" or become constant at about the same penetration distance for all applied currents with the exceptions of 10 and 20 mA, the largest currents. The penetration distance at which this leveling occurs, called the

penetration depth (Ref. 9), represents the distance over which the current is highest with corresponding higher polarizations and over which reaction intensity is also highest. The penetration depth is of practical significance because it can determine the practical thickness required for a "primary" electrode.

At the higher currents of 10 and 20 mA, larger penetration depths are obtained than for the lower currents because during the time of the potential-sweep measurements of each reference electrode, 10-15 seconds, a sufficient charge is passed to eliminate the secondary potential distribution initially present, yielding then a tertiary potential distribution. This shift in potentials and in the penetration depth, to larger values for the larger currents, 10 and 20 mA, is caused by precipitation of $Zn(OH)_2$ or ZnO on the frontal surface of the working electrode. This blockage then causes more reaction from the interior of the electrode, for constant applied total current, having the overall effect of increasing the penetration depth.

The primary penetration depth from Figures 4 and 5 is obtained by drawing a straight line from position No. 2 along subsequent potential values for all the applied currents with the exception of 10 and 20 mA which show secondary deviation behavior. The primary penetration depth is thus found to be 0.09 ± 0.01 cm, which agrees with the 0.09 cm previously reported (Ref. 1).

The semi-quantitative treatment developed by a host of workers has resulted in a generally accepted expression for penetration depth of electrochemical reaction (Ref. 9).

$$L = \left(\frac{RTc}{nFi_o \rho p} \right)^{1/2} \qquad (1)$$

Here, L is the primary penetration depth, c is the cross-sectional area of the pore, p is the pore's perimeter, and the other symbols have their usual meaning.

This expression must be applied carefully in terms of the experimentally determined penetration depth, L, because the expresion is an approximation. Also, changes in area, concentration, and morphology frequently shift L (Ref. 9), and successive reaction fronts may proceed along the pores (Ref. 27). Nevertheless, there are indications that the equation may be fairly accurate (Ref. 9), and it will be used in the following analysis.

The ratio of cross-sectional area, c, to perimeter, p, in our analog single-pore is esentially the pore height, t, and it can be shown that this is related to two very important parametric ratios in porous electrodes, pore volume to pore area, v/a, and fractional void volume to specific area, ε/A.

$$t = 2\frac{c}{p} = \frac{v}{a} = \frac{\varepsilon}{A} \qquad (2)$$

Considering conditions at room temperature and in 10 M KOH saturated with ZnO, those of our experiment, we obtain

$$L = \kappa\left(\frac{c}{p}\right)^{1/2} , \qquad (3)$$

and for $t = 20 \times 10^{-4}$ cm and L = 0.09 cm, we obtain

$$L = 2.0\left(\frac{\varepsilon}{A}\right)^{1/2} . \qquad (4)$$

From our routine examinations of commercially prepared electroformed, dendritic primary zinc electrodes we find that generally $\varepsilon = 0.75$ and $A = 5600$ cm^2. This yields from the above equation a primary penetration depth of 0.023 cm. Typically, commercial electrodes are about 0.01 cm thick, well within the range for optimal utilization of electrode area.

It may be reasonably considered that even secondary zinc electrodes should be thinner than the primary penetration depth to get the best performance, i.e., discharges relatively free of pore blockages that may arise in unduly long pores. For example, pore blockages can occur by ZnO or $Zn(OH)_2$ solid precipitate blocking the electrolyte path, by the same precipitate blocking the pore walls, and by electron-path blockage when dendrites are undercut during zinc dissolution. Conceivably, all of these deleterious effects are enhanced by pore lengthening beyond the penetration depth in secondary zinc electrodes.

2.3.1.2 Potential Distribution and Current

Examination of the potential distribution as current is varied by over 4 orders of magnitude, from 0.001 to 20.0 mA is of considerable interest for the case of secondary potential distribuiton. We note from Figures 4 and 5 that the polarization/distance curves within the pore are considerably removed from each other for currents from 20 to 1 mA, but for currents of 0.1 to 0.001 mA the polarization/distance curves are almost identical. How is this latter effect possible if the applied current is changed by two orders?

It appears that at the lower currents, 0.001 to 0.1 mA, the zinc electrode performs so well that the slight differences in polarization are hardly detectable experimentally. For example, if we plot the "Luggin potential" of the working zinc electrode, that is the potential at reference electrode position 1 which is 0.5 mm in front of the front edge of the working electrode, versus the applied current, then we observe constancy in this potential over a wide range, see Figure 6. In Figure 6 we plot both the Luggin potential and the estimated IR drop for the Luggin reference versus current.

It is apparent that at about 1 mA the IR drop becomes substantial with respect to the overall observed polarization of the working electrode, and thereafter for increasing currents and corresponding IR drops the working electrode polarization together increase in unison. It appears then that IR drop is a major factor in developing potential distribution once a certain value of current density is exceeded.

In our experimental arrangement the Luggin position (reference electrode 1) is 0.05 cm in front of the front edge of the working electrode while the penetration depth is 0.09 cm. The approximate coincidence of these two distances is an unexpected fortunate confirmation that the ohmic potential drop appears to dominate the current/potential behavior at currents higher than about 1mA as can be seen by comparing Figures 4 and 5 with Figure 6.

For the cross sectional current density with respect to the pore's cross section normal to the external current we have $1/20 \times 10^{-4}$ or 500 mA cm^{-2}, which is 1-2 orders of magnitude larger than current densities typical of polymer-bonded secondary zinc electrodes. For the current density on the zinc of the working electrode, assuming all of the current is averaged over the penetration depth, we obtain 1/0.09 or 11.1 mA cm^{-2}.

In general, if the polarization of a porous electrode changes only slightly over a wide applied current range, e.g., remaining at ca. 55 mV at 0.1 to 0.001 mA for our experiment, marked potential-distribution spreading by IR perturbations may be expected when the IR drop in the pore approaches the overall polarization of the pore. This occurs when

$$iL\rho \geq \eta \ . \qquad (5)$$

Here, i is the current density with respect to pore cross section and η is the persisting polarization.

2.3.1.3 Current Density and The Model Electrode

The analog pore electrode differs from real pores in porous electrodes in that its frontal area contains only the opening space without the adjacent solid sections. It is thus necessary to consider the frontal portion of a real electrode that is open or closed to ionic current when comparisons are made with the model.

The fraction of the electrode's exterior frontal surface area that is open to pores may be estimated by considering the surface of a plane through an electrode parallel to the electrode's frontal plane and having a solid area fraction θ. The fractional void volume of the porous electrode, ε, is related to both θ and the pore tortuosity τ

$$\varepsilon = \frac{\int(1 - \theta)\tau dX}{\int dX} = (1 - \theta)\tau \qquad (6)$$

The fraction of exterior frontal area that is open to pores may be taken as $1 - \theta$ or ε/τ, while the corresponding solid fraction of the exterior frontal area is θ. Typically, $\varepsilon \triangleq 0.75$ and $\tau \triangleq 3$ (Ref. 28) so that $1 - \theta$ is about 0.25, a small value compared to $\theta \triangleq 0.75$.

Thus, if an electrode's exterior frontal solid area becomes blocked by coverage with a masking reaction product during discharge, the actual current density at the open area may become 4-fold larger than the apparent exterior current density averaged over the entire electrode. Alternatively, during the inital stages of discharge the solid portions may concentrate higher current densities before they become blocked with reaction product. Interpretations of current density in the analog single-pore electrode should consider

this possible shifting of the division and wide variation of exterior current into the solid and open portions of the frontal area, i.e., compared to the averaged over-all current density, typically 10-100 mA cm^{-2}.

With the range of currents in the present work, 0.001 to 20 mA, the open-area current density at the mouth of the pore is determined by the cross section of the analog pore, 1 x 20 x 10^{-4} cm^2, to vary from 0.5 to 10,000 mA cm^{-2}. Considering possible external surface blockage this may correspond to as little as 1/4 less with respect to the superficial current density.

It should be noted that in commercial, electroformed zinc electrodes, a wide range in pore size and porosity can be typically observed so that most of the studied range in currents has practical import.

2.3.2 Evolution of Potential Profile

The evolution of potential profile with the passage of time is shown in Figure 7 for 1 mA of applied current. The potential profile is initially an exponential decrease from the front edge towards the interior of the pore electrode, as shown for the polarization/distance curve obtained after 25 seconds, Figure 7. However, after 100 seconds a change in the potential profile develops showing an increase in polarization at 0.8 mm and a decrease at 0.4 mm into the pore compared to the initially recorded curve. After 200 seconds this change becomes more pronounced indicating more polarization at 0.8 mm into the electrode than that near to the front edge.

This development of decreased polarization at the front edge of the electrode is evidently caused by blockage of the "second kind" when ZnO or $Zn(OH)_2$ precipitates on the zinc surface where the current density or reaction intensity was initially the greatest. After this partial blockage of the surface (see Ref.

25) at the front, the reaction intensity is greatest at some distance inward, i.e., 0.8 mm. It was previously shown that after 25 seconds ZnO deposits in the pore at distances up to 0.06 mm inwards and after 100 seconds the ZnO deposits up to 1.8 mm inwards (Ref. 1).

With the passage of time it is thus seen that the reaction can proceed to greater depths, drawing from the pore's interior. Most of the reaction activity, however, remained within a 1 to 2 mm penetration even after prolonged discharge, not much farther than the primary "penetration depth" of the potential profile, 0.9 mm.

It appears then that the primary penetration depth is a good indicator for an optimum electrode thickness for a zinc electrode, even though reaction activity develops inward into a porous structure. The inward development occurs at distances only slightly greater than the primary penetration depth and is accompanied by inefficiencies caused by internal ohmic resistance and pH change.

At smaller currents, 0.1 mA and less, there was little or no perceptible change in the potential profile with the passage of time for up to 1 to 2 hours, the maximum allotted time for this observation, see Figure 8. Evidently, at these lower rates sufficient time existed for diffusive relaxation of developed zincate and hydroxide ion concentrations so that precipitation blockage of the zinc surface was not appreciable.

During cycling at 0.1 mA it was typically observed that the cathodic potential profile decreased with the passage of time, Figure 9, relating to diminishing polarization within the pore. This behavior is attributed to the formation of zinc deposits which have greater surface area so that local current density actually decreases during the reduction. The penetration depth also appeared to become somewhat shorter at the same time, Figure 9, in accord with the effect of increasing specific surface area in Equation (1).

2.3.3 Edge Effects

By rotating the multiple reference electrode array, we could measure the potentials along the front edge of the zinc electrode from the corner inwards towards the center of the electrode as shown in Figure 10. It was considered important to measure this edge effect because of the findings of McBreen (Ref. 19) which indicated that shape change may be caused by concentration differences developed at the edge.

It should be noted that electrolyte creeps under the spacer on either side of the single-pore electrodes so that some current can leak in from the side edge of the electrode. It is estimated that the electrolyte film under the 15 micron thick spacer is about one micron thick. The distance between the top and bottom of the pore is 20 microns.

It is known that more current is drawn from the side edges because the reaction front moves in faster at the edges (Ref. 1). The overall geometric condition is not unlike that in a real cell where the edges of the zinc negative are exposed to electrolyte.

In Figure 11, we summarize all of the results for potential distribution at the edge inwards towards the center, see Figure 10 also. For currents of 0.01 mA and less there is essentially no edge effect, i.e., for frontal current densities of about 5 mA cm^{-2} or less. It is striking, however, that with increasing current above 0.01 mA an edge effect develops, and the primary penetration depth increases, from about 2 to 5 mm, as current is increased from 0.05 to 1.0 mA or from 25 to 500 mA cm^{-2} in frontal current density.

The elementary theory (Ref. 9) predicts that the primary penetration depth into the pore be independent of frontal current density for small currents as was found and shown in Figure 5. Here, the current leaking in from the side edge must be increasing with higher applied overall currents causing the primary penetration depth to be dependent on the current.

It thus appears that edge effects will be larger for larger currents and below a certain minimum current density, 5 mA cm^{-2} for our pore, edge effects become unimportant.

2.3.4 Concentration Profile

It has been shown by Bode et al (Ref. 24) that the potential of the zinc electrode in an alkaline zincate-ion solution is dependent only on the OH^- concentration. Bode et al assumed that equilibrium was established between ZnO and the electrolyte and applied the solubility product of ZnO to the Nernst equation to show that the equilibrium potential for Zn is displaced by an amount dependent on 0.059 log (OH^-).

In the work reported here in Figure 12, however, we utilized results obtained earlier (Ref. 2) with Zn/Zn concentration cells to obtain an estimate of the OH^- concentration. In this way liquid junction potentials are taken into account. It was found that the potential difference between two zinc electrodes varied linearly with OH^- concentration at 21.9 mV/M(OH^-) in the range of 7.7 to 10 M KOH as zincate ion was reduced from 1.14 to 0 M, at 22.3°C. These conditions closely approximate those existing in the single-pore electrode between the multiple array of zinc electrodes and the working zinc electrode.

The use of the concentration cell empirical data rather than the Bode et al approximation (Ref. 24) resulted in a less severe apparent change in OH^- concentration. The latter approximation yields about 4.0 mV/M(OH^-).

In Figure 12, then, we show the open-circuit potential profiles and the estimated concentration profiles for OH^-. These curves were obtained 25 and 600 seconds after the working electrode was held at 1 mA of closed-circuit anodic current for 86 seconds. After 86 seconds at 1 mA only a small fraction of the OH^- within the pore volume is consumed by formation of $Zn(OH)_4^=$, and it can be estimated that diffusion to the reference electrodes is also small.

From Figures 12 and 7 it appears that the (OH^-) actually increases from 7.7 M to values of about 8.4 M or more at the pore mouth because a substantial amount of ZnO is precipating.

$$Zn\ (OH)_4^= \ = \ ZnO + H_2O + 2OH^-$$

This would explain the observed increase in (OH^-), Figure 12, and the shift in potential profile. Figure 7.

In the interior of the pore the (OH^-) decreases from the initial 7.7 M to 7.4 M or less, because of zinc dissolution

$$4OH^- + Zn \ = \ Zn(OH)_4^= + 2e^-$$

After the passage of 600 seconds, the concentration profile is somewhat relaxed, but it still persists, suggesting that diffusional relaxation is relatively slow and that the data collected after 25 seconds, Figure 12, is reasonably representative of the initial condition.

From the magnitude of the potential differences manifested across the electrode initially at open circuit, up to 15 mV, and from the persistence after 600 seconds, to about 7 mV, we may anticipate a flow of current across the electrode. From our data on concentration cells (Ref. 2), currents of about 0.2 to 0.4 $mAcm^{-2}$ may be anticipated with dissolution of zinc at the high (OH^-) regions and the deposition of zinc at the low (OH^-) regions.

This latter behavior suggests that regions of a zinc electrode that experience relatively high discharge currents, e.g., the edges, develop a more negative open-circuit potential during and after the discharge, relative to those at regions of lower current densities.

This effect may contribute to shape change as well as the diffusion of zincate ion away from regions of high current density as indicated by McBreen (Ref. 19).

The data of Figure 12 were obtained with zinc reference electrodess in the multiple array. This reference electrode system crazed and cracked after one week of usage in the alkaline electrolyte because of the sharp edges on the alumina plate substrate. A new multiple reference electrode was then prepared using vapor deposited silver instead of zinc, relying on the Ag_2O/Ag reference potential. This electrode utilized an alumina plate with rounded edges so that the crazing problem was prevented.

In Figure 13 we see the results of cycling the working zinc electrode at 1 mA with 120 seconds on discharge and then 120 seconds on charge for 5 cycles. Open-circuit potentials were recorded immediately after discharge and then after charge. It can be seen that the regular trend in potentials (and concentrations of OH^-) after 86 seconds, Figure 12, are not held as well after 120 seconds for the discharge curve. Apparently, precipitation of ZnO and the release of OH^- can occur preferentially at different sites within the first 2 mm of pore depth, as indicated by the shifts in potential to more negative values, Figure 13.

It is interesting that during cycling the frontal region of the electrode has positions that are generally more negative than the interior and thus contain more OH^- during open circuit after either charge or discharge, Figure 13. After charge the overall

electrode potential is usually at -1.26V (S.H.E.), and after discharge the overall potential is about -1.23V (S.H.E.) in keeping with an overall generation and decrease in (OH^-), respectively. As the electrode is cycled it's open circuit potential can change by as much as 40 mV, corresponding to an OH^- concen-tration change of about 40/21.9 or 1.8 M OH^-, vide infra.

At lower current, 0.1 mA, similar behavior is observed for the open-circuit potential and concentration profiles. In Figure 14 we observe the change in open-circuit overall potential of the working zinc electrode at various times during cycling at 0.1 mA. For the prolonged cycle times used here, up to 20 minutes on discharge, we note that the open-circuit potential can vary by 85 mV, corresponding to 85/21.9 or 3.9 M OH^-.

For the first discharge and second charge shown in Figure 14, the open-circuit potential profiles are plotted at the beginning and end of the discharge and charge in Figure 15a and 15b. Here, it is apparent that OH^- concentration changes throughout the pore in accord with the observed overall potentials. Hydroxide ion is consumed during discharge and released during charge. Again, the pore appears to be more negative in the first 2 mm of the frontal region after either charge or discharge.

The behavior observed with these open-circuit potential profiles showing potential shifts and OH^- concentration persisting at the first 2 mm of the frontal edge, suggests that concentration cells will always be formed on cycled zinc electrodes if the current distribution is not uniform. Further, the concentration cell would act to cause zinc dissolution at the frontal edge and zinc deposition inside the pore. This is exactly what was observed in a previous study (Ref. 2). Zinc metal movement within the pore was from the frontal edge towards the interior as shown in Figure 16. The cell was cycled at 60 seconds, 2 mA, anodic and 60 seconds, 2 mA, cathodic.

Similar behavior may be expected at the edges of a zinc electrode when current densities are high enough to cause appreciable edge effects, and, in general, in closed, compact systems migration of metallic zinc should always be towards regions experiencing the lowest current density on charge and discharge (Ref. 29), as indicated in Figure 17.

It should be noted that the concentration-cell effect would act immediately whereas diffusive migration of zincate ion appears to be too slow to explain shape change. For a typical edge effect of 15 mV (Figure 12) we can anticipate a concentration-cell current density of 0.4 mA cm^{-2} (Ref. 2). Assuming that this current acts mostly during the discharge periods at a typical overall current density of 150 mA cm^{-2}, then the concentration-cell edge effect currents would become competitive after 150/0.4 or 375 cycles which is on the order of the observed maximum possible cycles.

To prevent shape change caused by these edge effects, electrode designs should be utilized that distribute the current more uniformly. Possible designs are (1) the use of separators with less porosity at the electrode's edges, (2) the use of substrates with more ohmic resistance at the edges, (3) the use of smaller counter electrodes, and (4) roughening the edges of the zinc substrate at the edges.

Section 3
PLANAR ELECTRODE STUDY

3.1 INTRODUCTION

The literature of shape change has been reviewed by Sunu and Bennion (Ref. 30). Generally, two effects that cause shape change are cited; that caused by increased current to the edges, with subsequent inward diffusion in zincate ions (Refs. 19, 31, 32) and that caused by electroosmosis (membrane pumping) with convective movement of zincate inwards to supplant the "pumped" electrolyte (Refs. 33, 34). Both effects appear to have been demonstrated experimentally (Refs. 19, 8).

Some question exists, however, on the relative magnitudes of each effect as well as upon their efficacy. Concentration gradients of zincate ion were shown to be relieved at effective rates through the zinc by electrical current developed from the resulting concentration cell (Ref. 2 and Section 2.3.4), possibly circumventing the diffusion process. Independent experimental tests of the membrane pumping effect have not always been favorable (Ref. 35).

Further, the possibility of other contributing processes must, at least a priori, be considered. We may summarize some of these possibilities known to the electrochemical engineer.

1. Edge effects, described above.
2. Electroosmotic pumping, described above.
3. Surface tension effects. These may be caused by the pronounced increase in surface tension with increase in OH^- (Ref. 36). Concentration gradients can induce motion through the capillary pores of the electrode or space between membrane and electrode (e.g., Ref. 37).

4. Electrophoretic effects. Microscopic observations of hydrogen bubble and ZnO movement have indicated a rapid, impelled-type of movement (Ref. 25). The former may cause convection, the latter, Zn migration additionally (Ref. 38).
5. Concentration cell effects. Concentration cells, with alkaline-zincate ions, discharge with formation of mossy zinc (Ref. 2). The mossy zinc is, in turn, unstable with respect to corrosion by electrolyte (Ref. 2). These steps may be involved in the overall mechanism of edge effects
6. Osmosis. Water is generally consumed at the postive and formed at the negative during discharge. This situation, together with the formation of zincate ion, may develop substantial osmotic pressures with resultant convective flows.
7. Electrochemical Displacement. Isolated zinc particles in aqueous 10M KOH solution, saturated with ZnO, can move by electrochemical displacement in an electric field (Ref. 39). Zinc deposits from the electrolyte on one side and undergoes dissolution on the other side of the particle causing an overall movement.

As noted in Section 2, edge effects combined with concentration-cell effects appear to be of the correct order of magnitude to cause shape change. It appears warranted to consider these effects further.

Surface tension in the maximum anticipated range of KOH concentration change, from 10M KOH to 7.49M KOH, for zincate-ion free electrolyte to supersaturated zincate-ion electrolyte (Figure 12 and Ref. 2) should vary from about 96 to 90 dynes cm^{-1} (Ref. 39), i.e., by only a 6 dynes cm^{-1} difference, assuming zincate ion has only a small effect. This does not appear to be a large enough difference to cause appreciable convective flow (see Ref. 37).

Isolated zinc particles are generally not found in sufficient amounts at zinc electrodes so that electrophoresis and electrochemical displacement do not appear to be responsible phenomena for shape change. Further, the motions are generally too slow to cause serious concern (Ref. 38).

Finally, electroosmosis and osmosis may possibly be governing processes for shape change because of the rapid convective movement induced through cellophane membranes in discharging electrochemical systems containing alkaline aqueous electrolyte and zinc negatives. This induced electrolyte motion during discharge can be readily demonstrated (Ref. 30), and only a minute convective motion between the faying surfaces of the separator and electrode lateral to overall current flow can cause relatively large lateral gradients in zincate ion.

It is important, then, to undertake a series of elementary experiments to seek and evaluate the above candidate processes that induce shape change in the zinc electrode. Especially, it is important to compare the most likely processes, edge concentration-cell effects and osmotic pumping effects. For this task the use of two conforming, planar electrodes is well suited.

In this section we describe these experiments with planar electrodes. A thin coating of zinc is electroplated onto a flat polished silver electrode and the movement of the zinc is observed as this electrode is cycled either with an open area between the electrodes (edge concentration-cell effects) or with a cellophane membrane between the electrodes (osmotic effects). The movement of the zinc on the silver surface can be readily observed because of the contrast in appearance of the polished, flat silver surface and the various morphological forms of deposited zinc. Effects in the direction lateral to overall current flow are isolated and enhanced because of the minimization of electrode depth. A considerable depth of cycling can be affected within a short time, a few minutes, because of the thin zinc coating, and this allows attainment of cycle numbers approaching 1000 in one day so that observation times can be greatly reduced compared to real electrodes.

3.2 EXPERIMENTAL

The working electrode consists of a 1x1x0.3 cm silver slug embedded in a 1-inch diameter epoxy cylinder as shown in Figure 18. The cylinder is 1.4 cm long and fits into a metallurgical fixture for polishing the exposed 1x1 cm surface on a polishing wheel. Electrical connection is made to the electrode with a bolt through a threaded hole on the opposite side of the cylinder. Before an experiment the silver surface is electroplated with zinc in a 10M KOH solution saturated with ZnO for 9 seconds at 150 mA. This corresponds to a thickness of $(9x150x10^{-3}x65.38)/(96,520x2x7.14x1)$ or 0.64 micron. Electroplating is versus an oversize platinum screen placed parallel and adjacent to the exposed silver surface.

During an experiment, an electrolyte dam is formed around the edge of the cylinder with all-Teflon plumber's tape. Electrolyte, 10N KOH, saturated ZnO, is then added to cover the working electrode with a few mm of electrolyte. The separator and counter electrode are placed on the electrode, Figure 18, and a glass weight is placed on top to press the counter electrode to the zinc electrode.

The counter electrode is a commercial 1x1 cm $Ag/Ag_2O/AgO$ electrode about 1 mm thick and containing about 0.4 AH cm^{-2} of charge. The counter electrode thus contains ample capacity to never be limiting in the preselected sequence of experiments.

A needle Luggin probe, previously described in the literature (Ref. 25), is placed near the edge of the two electrodes, and the system is cycled at 100 mA, 9 seconds on discharge and 150 mA, 6 seconds on charge. This corresponds to a 67 percent depth of discharge with equal coulombic charge and discharge. Before cycling, the working electrode always appeared smooth with a dull gray zinc coloration. Unless otherwise noted, all cycling was under these conditions.

3.3 RESULTS AND DISCUSSION

3.3.1 Cycling Behavior

Typically, cycling caused a gradual improvement in performance as marked by a gradual decrease in polarization during discharge until about 15 cycles when the polarization started to remain constant with cycle number. This behavior is shown in Figure 19 for an electrode charged at 150 mA, 9 seconds, and then cycled at 100 mA, 10 seconds each half cycle. An open, 10-mesh grid made from 20-mil polypropylene threads was used as the separator.

This gradual improvement during the first few cycles is attributed to a "breaking-in" period when morphological adjustments are made. During the cycling the surface visually appears to become roughened, and it is believed that more nucleation sites are formed each cycle until a quasi steady-state exists, and surface area no longer increases with continued cycling.

If cycling is initially conducted at a somewhat lower current density, then the electrode may be made smoother with each cycle, and the polarization can actually increase with cycle number before leveling off to a constant value. This behavior is shown in Figure 20 for an electrode charge at 150 mA, 9 seconds, and then cycled at 35 mA, 30 seconds each half cycle. The same, open-structured polypropylene grid separator was used as for the experiments of Figure 19.

It is apparent that considerable insight can be obtained on the importance of morphology by conducting experiments where the initial current density is varied, and then observing the change in polarization during cycling at various current densities. Such experiments would be of value if they included charging in a mossy zinc regime (low current densities), and introducing a wet stand before discharge.

With experiments reported here, 35 to 150 mA of deposition current, the zinc deposits always appeared smooth with a dull gray color.

The results of Figures 19 and 20 lead to the suggestion that charging should be conducted at as high a current density as practically possible without developing hydrogen evolution that would be detrimental to the system. In this way, relatively high surface-area zinc dendrites can be formed which would greatly improve discharge performance by decreasing polarization.

The instability of mossy zinc towards corrosion during wet stand was shown previously (Ref. 2), and charging current densities that are so low that mossy zinc can be formed are best avoided. Otherwise, the deposited mossy zinc may undergo dissolution.

The current densities at which a transition occurs from mossy zinc to boulder or smooth zinc, from smooth to dendritic zinc, and from dendritic zinc to frank hydrogen evolution should be determined for each static, secondary alkaline zinc system. Charging then should be carried out in the dendritic regime if a stable, high surface area deposit is required.

Transition current densities for zinc will depend on concentrations, temperature, and the specific geometrical constraints of the system. For an isolated zinc particle in a capillary with 10 M KOH saturated with ZnO, we found that a mossy to dendritic zinc transition occurs at 200 mA cm^{-2} and frank hydrogen evolution at 1200 mA cm^{-2} (Ref. 2). With a small-scale, production-type plating bath we found a transition from smooth, boulder-type zinc to dendritic zinc at 100 mA cm^{-2} for 6.5 M KOH containing 0.5 M ZnO.

3.3.2 Open Structure

The planar zinc electrode was cycled with the relatively open structure of 10-mesh, 20 mil woven polypropylene used as a separator. After 1000 cycles the planar zinc surface was examined at 70x.

Typically, zinc disappeared from a region extending to about 0.5 mm from the edges and 1.0 mm from the corners of the square electrode. The existence of an edge effect in a non-compact configuration was thus definitely established.

Further, it was observed that mounds of zinc formed wherever the polypropylene 10-mesh grid touched the planar electrode's surface, Figure 21a. A pattern of zinc was formed matching the 10-mesh grid. This confirms the findings noted in Section 2.3.4 and Figure 17 that metallic zinc always migrates to regions that experience the lowest current density during cycling. Wherever the grid touched the planar electrode the current density was decreased because of increased IR drop in the electrolyte between the faying surfaces.

3.3.3 Displaced Electrodes

In one set of experiments the upper AgO counter electrode was displaced sideways so that it only covered half the lower zinc electrode, and the 10-mesh polypropylene separator was used. The cell was given 1000 cycles and examined at 70x. Most of the zinc migrated away from the area where the silver counter electrode covered the zinc electrode, and a layer of zinc was formed where the zinc electrode was not covered by the counter electrode, Figure 21b.

Again, the zinc is shown to migrate to regions experiencing the lowest current densities. The uncovered portions of the zinc electrode were farther removed from the counter electrode and thus would experience less current.

3.3.4 Separator Paper

The cell was cycled with separator paper as a separator rather than the 10-mesh polypropylene. The separator paper had a fine, porous structure as shown in Figure 22. After 1000 cycles it was found that the edge effects observed with the 10-mesh grid were nearly absent. Only a small amount of migration could be seen, to about 0.1 mm. Apparently, the added separator paper imparts extra ohmic resistance between the electrodes so that less current is preferentially directed to the edges of the working electrode.

3.3.5 Regenerated Cellulose

When the separator was replaced with commercially prepared regenerated cellulose (cellophane) wrapped around the counter electrode, failure occurred after only 15 to 20 cycles because of excessive polarization. Examination of the zinc electrode

revealed that it was almost bare of zinc, with most of the silver substrate exposed, Figure 21c. This effect is appearently caused by an osmotic pumping across the membrane towards the zinc electrode so that the discharged zinc, in the form of zincate ion is swept away from between the electrodes. During charge there is then successively less zincate ion present to enable adequate deposition.

When the experiment was repeated with a regenerated cellulose separator punched about 100 times with a pin to allow convective flow back to the counter electrode, the same failure occurred after 20 cycles with a resulting similar-appearing bare silver surface. Evidently, the pin holes presented too much resistance to electrolyte flow compared to the sideward direction flow away from the electrodes.

From the results of these experiments, it appeared important to determine whether the induced flow was osmotic or electroosmotic or both. The experiments of Section 4 were designed to evaluate these processes.

3.3.6 Larger and Smaller Counter Electrodes

Edge effects occur because of the higher current densities at the edges as noted in Section 2.3.4 and Figure 17. To further corroborate this notion, we prepared counter electrodes which were larger and smaller than the working electrode, 1.1 x 1.1 cm and 0.9 x 0.9 cm, respectively. We then cycled the cell with the separator paper present.

As anticipated, with a larger counter electrode yielding more current to the edges a drastic shape change occurred. With the smaller counter electrode zinc was actually drawn to the edges, Figures 21d and 21e. These results confirmed the previous findings and suggested that a smaller counter electrode would be beneficial in practice.

3.3.7 Roughened Edge Electrode

In one experiment a 1-mm wide region along the edges of working electrode was abraded with 600 mesh sandpaper. This served to decrease the local current density at the edges. The abraded electrode was then cycled with separator paper between the electrodes and no edge effects were present after 1000 cycles. Evidently, the abrasion roughened the surface enough to decrease the edge's local current density and prevent the effect noted in Figure 17.

Section 4
OSMOTIC EFFECTS

4.1 INTRODUCTION

It has been established that convective movement of electrolyte proceeds through regenerated cellulose or cellophane membranes during discharge of alkaline zinc electrodes (Refs. 33, 34). Further, in the work reported here (Section 3.3.5) there does appear to be a net flow towards the zinc electrode during cycling.

The regenerated cellulose membrane may be considered as a semi-permeable membrane, and as such it may be expected to develop osmotic flow. As indicated in Section 2, we can anticipate the formation of concentration gradients in OH^- and $Zn(OH)_4^=$ across the membrane. Furthermore, we have found in commercial cells that there may be only 20 percent of the required OH^- present in the electrolyte to discharge the zinc so that OH^- concentration gradients can be large. Osmosis then may occur and may be more significant than electroosmotic or electrokinetic pumping through the membrane. The experiments reported in this section were conducted to determine the relative magnitudes of osmosis and electroosmosis to identify the cause of the failures of our cell when we cycled it with reconstituted cellulose, to guide cell development.

We placed electrolyte in a container of fixed volume with a calibrated capillary tube housing the meniscus and with a membrane at one end of the container. We then exposed the membrane either to electrolytes of differing concentrations or of the same concentration while passing current through the membrane. The movement of the meniscus could then be related to the rate of the manifested process.

4.2 EXPERIMENTAL

The osmosis cell consisted of a 4-cm length of 8-mm OD Pyrex tubing fused to the end of a 19-cm length of 1-mm ID Pyrex capillary tubing as shown in Figure 23. A hole was blown in the 8 mm tubing, and a commercial $Ag/Ag_2O/AgO$ electrode was placed in the tube with a platinum lead wire passing through the hole and sealed with epoxy at the hole. The capillary tube had 1 mm graph paper attached for measuring rate, and the reconstituted cellulose was attached to the end of the 8 mm tube with "O" rings after the membrane was soaked overnight in electrolyte.

During an experiment the end with the membrane was placed in a beaker of the same electrolyte as in the cell and current was passed first in one direction then in another through the membrane to a counter electrode of platinum gauze in the beaker. For osmosis experiments no current was passed but the membrane was placed in first the same electrolyte and observed, and then in another electrolyte. The dissimilar electrolytes were then exchanged to assure that a gravity effect was not significant.

Care was taken to place the meniscus of the liquid in the cell at the calibrated portion of the capillary tube so that its movement could be recorded and timed with a stop watch. The 8-mm Pyrex tube had a 0.55-cm ID, corresponding to an area of 0.24-cm^2.

4.3 ELECTROOSMOSIS

The cell was assembled with its end in a beaker and with 9.7 M KOH in the cell and in the beaker. The membrane was soaked overnight in the 9.7 M KOH.

Current was forced past in the sense that the silver electrode was discharged (reduced). Current was held at 0.1, 1.0, and 24 mA for periods up to 10 minutes with no perceptible movement of the meniscus. No movement was observed when the currents were

reversed for similar time periods. For a 5 minute period the membrane sustained 48 mA of silver electrode discharge, again with no perceptible movement.

Under the conditions of the experiment the constructed cell was not sensitive enough to detect any occurrence of electroosmosis. It is estimated that the meniscus could be recorded to ± 0.01 cm in the capillary, and for a 10 minute period this corresponds to the observation that electroosmosis effects result in electrolyte flow at a rate less than $1.3 \times 10^{-7} cm^3 cm^{-2} sec^{-1}$ at 100 mA cm^{-2}.

4.4 OSMOSIS

The cell was assembled with 10 M KOH saturated in ZnO and with the membrane soaked overnight in this electrolyte. The end with the membrane was placed in 10 M KOH in a beaker and the meniscus was observed.

The meniscus moved in the sense that flow was towards the 10 M KOH, saturated ZnO, and away from 10 M KOH. Nine measurements were made corresponding to a flux through the membrane of $(9.0 \pm 1.5) 10^{-6} cm^3 cm^{-2} sec^{-1}$. The experiment was repeated with similar results.

In another set of experiments the cell again contained 10 M KOH saturated in ZnO but the end was placed in a beaker of water. The osmotic flow was towards the 10 M KOH, saturated ZnO, at a rate of $(151 \pm 15) 10^{-6} cm^3 cm^{-2} sec^{-1}$, averaged from 11 measurements.

It appears that osmosis is much faster than electroosmosis in our electrochemical systems. If practical cells are starved in OH^-, then osmotic rates can be fairly high, approaching $150 \times 10^{-6} cm^3 cm^{-2} sec^{-1}$. For tightly packed electrodes this can cause considerable sideward flux. From the general appearance of concentration profiles described in Section 2 it may be anticipated that osmotic flow during discharge will be faster at the edges of the electrode.

The significance of the osmotic flow can be judged from a calculation of the total osmotic flow required to carry away a saturated solution of $Zn(OH)_4^=$ containing all of the electrode. By comparing the time required for this process with the time for each cycle we can estimate the minimum cycles to effect shape change:

Basis 1 cm^2 of electrode area:

Electrode thickness, 1 mm; 70% porosity; 100 mA cm^{-2} discharge C.D.; M. W. Zn, 65.4; density Zn, 7.14; depth of discharge 100%; 2 equiv./mole; 96,520 coul./equiv:

$$\text{Time}_{\text{per cycle}} \text{ of discharge} = \frac{0.1(7.14)0.3x2x96,520}{65.4x100x10^{-3}} = 6.4x10^3 \text{ sec cycle}^{-1}$$

Assume 1 M $Zn(OH)_4^=$ and $10^{-5} cm^3 cm^2 sec^{-1}$ osmosis:

$$\text{Time to develop sufficient electrolyte to remove all zinc} = \frac{0.1(7.14)x0.3x1000}{65.4x1x10^{-5}}$$

$$= 3.3x10^5 \text{ seconds}$$

$$\text{No. cycles} = \frac{3.3x10^5}{6.4x10^3} = \underline{52 \text{ cycles}}$$

Thus, it can be seen that if the depth of discharge is less than 100 percent, the estimated 52 cycles to failure could easily become larger to approach the commonly observed 200 to 300 cycle life.

It was shown that shape change can occur without a semi-permeable membrane, Section 2.3.4, and it thus appears that both processes can act and are of the same order of magnitude.

Section 5
SUMMARY AND CONCLUSIONS

Studies were conducted to ascertain causes of zinc shape change using analogs of specific components of the zinc electrode/electrolyte/separator system in a typical porous electrode system in secondary applications. The concentration and polarization profiles within the minute confines of a zinc pore were examined, the possible magnitude of edge effects were determined, and the influences of current distribution and cellophane separator material on the movement of zinc during cycling, i.e., shape change were found.

For these studies, three well-characterized configurations of specific parts of a real electrode system were used. A model pore, 20-micron wide, was probed with six reference electrodes along the first millimeter into the pore to measure polarization and concentration. Second a planar electrode was studied with and without a cellophane separator and in various positions with respect to the counter electrode. This analog was used to find the effects of osmosis with a semi-permeable membrane present and, without the membrane, to determine the direction of zinc movement or shape change with respect to current distribution during cycling. Third, a simple, osmotic cell was assembled to determine whether electroosmosis (electrokinetic motion) or osmosis governed the previously reported convective motion and to ascertain the direction of the osmotic processes.

During the course of these studies it was found that both osmosis and current distribution effects could cause shape change, and, further, both had the same order of magnitude in influencing the change. Other conceivable processes, including electroosmosis, were not as important as osmosis or current distribution and could be disregarded in considerations of a corrective action.

Other conclusions were made as a result of this study using 10 M KOH electrolyte:

1. During cycling the overall (Luggin) open-circuit potential of the zinc electrode oscillates by 85 mV, being more positive during discharge and more negative during charge, while the applied discharges and charges are held at 0.1 mA (50 $mAcm^{-2}$) for up to 20 minutes, Figure 14.
2. The changes in electrode potential during cycling are caused by the overall consumption of OH^- during discharge and its release during charge. From previous concentration cell studies (Ref. 2), the 85 mV shift in open-circuit potentials is determined to be caused by a 4.0 M shift in OH^- concentration.
3. During cycling, within the region extending to 1 mm from the front edge of the pore, the potential is generally more negative than at a distance farther into the pore. This effect is caused by the relatively large amounts of precipitated ZnO which releases OH^- at this location. During charge, all of this precipitated ZnO is not reduced, leaving the frontal region slightly more negative in potential compared to the interior, Figures 13 and 15.
4. Careful measurements of the open-circuit potential profile after a single discharge at 1 mA (500 mA cm^{-2}) for 86 seconds demonstrated that potentials at the front edge of the pore could indeed be 20 mV more negative than in the interior of the pore and 15 mV more negative than the original rest-potential value. This indicates that a concentration shift from 7.7 M OH^- to 8.4 M OH^- takes place at the front edge while OH^- decreased from 7.7M OH^- to 7.4 M in the interior of the pore, Figure 12. Thus, overall concentration differences of 1M in OH^- can occur within a pore.
5. The cycling process is not 100 percent efficient, and this may perpetuate the OH^- concentration gradient within a pore.
6. The formation of OH^- gradients at the edges, lateral to overall current flow, should occur as indicated because of the increased current at the edges, Figure 11. It was shown

that concentration cells can produce current densities on the order of 0.4 mA cm^{-2} which will become coulombically comparable to a single cycle after a few hundred cycles of operation. Edge effects can thus account for shape change.

7. It was demonstrated with cycled planar electrodes that edge effects alone cause shape change.
8. The penetration depth for the current distribution within a pore parallel to overall current direction does not change over a wide range of currents, 0.001 to 7.5 mA, corresponding to 0.5 to 3750 mA cm^{-2}, respectively, Figures 4 and 5. The penetration depth for the current distribution perpendicular to the overall current direction changes markedly once a minimum overall current density is exceeded, Figure 11.
9. Once the IR drop through a pore becomes comparable with the overall polarization of the electrode, marked differences in the pore's current distribution will develop when the overall current density is increased. It appears that the IR drop is then essentially controlling the overall polarization.
10. Zinc electrodes having the characteristic dendritic structure should be no more than 0.02 cm thick for maximizing efficiency. For other structures this thickness should be no more than about $2(\varepsilon/A)^{1/2}$ where ε and A are the fractional void volume and specific surface area, respectively.
11. In general, zinc electrodes will change their shape during cycling such that zinc accumulates where local current density was least. Cell designs should thus be made to make electrode current density more uniform.
12. Two designs that were shown to counter shape change were (1.) using a smaller counter electrode and (2.) roughening the edges of the electrode's substrate.
13. The presence of a semi-permeable membrane separator will generate strong convective flow that will be responsible for shape change.
14. In the case of reconstituted cellulose (cellophane), osmosis is the process that causes strong convective flow and not electroosmosis.

Section 6
RECOMMENDATIONS

In view of improvements over the shape-change effect obtained in a few preliminary experiments resulting from this work, it is recommended that development work be started with zinc electrodes in static electrolyte systems.

As noted, however, the zinc electrode development will incur certain inherent requirements. The presence of a semi-permeable membrane separator induces osmotic flow even when it is perforated. It may thus be necessary to use only a porous separator. If this is acceptable then charging currents should be just below the hydrogen evolution limit to prevent dendritic shorting and above the mossy zinc limit to prevent corrosion on wet stand. Further, the maintenance of a uniform current density across the electrode lateral to current flow will be a necessity.

Recommendations for developmental work may be found throughout this report, but the more important issues are summarized below.

1. Semi-permeable membrane separators should be avoided.
2. Lateral current distribution should be uniform.
3. Uniform lateral current distribution can be obtained by roughening the substrate edges or by using a smaller counter electrode, as shown in the preliminary experiments. Other design suggestions are (a) graded porosity in separator material, (b) graded ohmic resistance or porosity of substrate, and (c) graded porosity of counter electrode, such that less current is drawn from the edges.
4. Electrodes should be about 0.02 cm thick or less if a typical dendritic structure is utilized. Otherwise, for a structured substrate the formula given in the text should be used.
5. Consideration should be given to using a high concentration soluble zinc salt or complex in the solution to avoid difficulties arising from ZnO precipitation.

6. Charging current should be carefully controlled to avoid hydrogen evolution and mossy zinc formation.
7. Precision cell construction is needed with uniform electrode spacing.

Section 7
REFERENCES

1. T. Katan and P. J. Bergeron, Basic Studies on Nickel-Zinc Batteries, Lockheed Missiles & Space Company, Inc., Sunnyvale, CA, DOE Contract EM-78-C-01-565, 28 November 1979.

2. T. Katan, P. J. Carlen, and R. F. Srna, Basic Studies on Nickel-Zinc Batteries, Lockheed Missiles & Space Company, Inc., Sunnyvale, CA, DOE Contract S/C 4503610, 30 August 1981.

3. A. R. Landgrebe, K. Klunder, and N. P. Yao, Proceedings of 27th Power Sources Symposium, 1976, p. 23.

4. L. E. Miller, and R. A. Brown, Ibid., p. 16.

5. S. Font and J. Goualard, "Power Sources 5," Proceedings 9th International Symposium, D. H. Collins, ed., Brighton, England, Academic Press, 1974.

6. J. J. Lander, in Zinc-Silver Oxide Batteries, A. Fleischer and J. J. Lander, eds., New York, John Wiley & Sons, Inc., 1971, p. 457.

7. S. U. Falk and A. J. Salkind, Alkaline Storage Batteries, New York, John Wiley & Sons, 1969.

8. U. S. Bagotzky and A. M. Skundir, "Chemical Power Sources", p. 246, Academic Press, New York, (1980).

9. S. Szpak and T. Katan, Proc. Symp. on Electrode Materials and Processes", The Electrochemical Society Proceedings Vol. 77-6, 770 (1977).

10. R. C. Alkire, E. A. Grens, and C. W. Tobias, J. Electrochem. Soc. 116, 1328 (1969).

11. P. Bro and H. Y. Kang, J. Electrochem. Soc. 118, 519 (1971).

12. Z. Nagy and J. O'M. Bockris, J. Electrochem. Soc. 119, 1129 (1972).

13. D. Simonsson, J. Electrochem. Soc. 120, 151 (1973).

14. T. Katan, H. Gu, and D. N. Bennion, J. Electrochem. Soc. 123, 1370 (1976).

15. W. Sunu, Ph.D. Thesis, Department of Engineering, UCLA (1978).

16. S. Szpak, J. D. Elwin, and T. Katan, Electrochem. Acta 11, 934 (1966).

17. J. J. Coleman, J. Electrochem. Soc. 98, 26 (1951).

18. E. C. Gagnon and L. G. Austin, J. Electrochem Soc. 118, 497 (1971).

19. J. McBreen, J. Electrochem. Soc. 119, 1620 (1972).

20. S. Szpak and T. Katan, J. Electrochem. Soc. 122, 1063 (1975).

21. M. B. Liu, Y. Yamazaki, G. M. Cook, and N. P. Yao, "Transient Current Distributions", ANL/OEPM-80-6 (1981).

22. R. J. Brodd, Electrochim. Acta 11, 1107 (1966).

23. J. H. Flatt, F. R. McLarnon, and E. J. Cairns, "Optical and Electrochemical Study of Model Zinc Electrode Pores In Alkaline Electrolytes", Abstract 825, 163rd Meeting, Electrochem. Soc., May 8-13, 1983.

24. H. H. Bode, V. A. Oliapuram, D. Brendt, and P. Ness, in "Zinc-Silver Oxide Batteries", A. Fleischer and J. J. Lauder, eds., John Wiley & Sons, Inc., New York, 1971.

25. T. Katan, J. R. Savory, J. Perkins, J. Electrochem. Soc. 126, 1835 (1979).

26. J. Newman and W. Tiedeman, AIChE Journal, 21, 25 (1975).

27. S. Szpak, A. Nedoluha, and T. Katan, J. Electrochem. Soc. 122, 1054 (1975).

28. T. Katan and H. F. Bauman, J. Electrochem. Soc. 126, 1835 (1979).

29. F. McLarnon, private communication, June 1984.

30. W. G. Sunu and D. N. Bennion, J. Electrochem. Soc. 127, 2007 (1980).

31. G. A. Dalin, in "Zinc-Silver Oxide Batteries," A. Fleischer and J. J. Lander, Editors, pp. 87-95, John Wiley & Sons, Inc., New York (1971).

32. J. McBreen and G. A. Dalin, Paper 45 presented at The Electrochemical Society Meeting, Philadelphia, Pennsylvania, October 9-14, 1966.

33. K. W. Choi, D. N. Bennion, and J. Newman, J. Electrochem. Soc. 123, 1616 (1976).

34. K. W. Choi, D. Hamby, D. N. Bennion, and J. Newman, ibid., 123, 1628 (1976).

35. D. Hamby and J. Wirkkala, ibid., 125, 1020 (1978)

36. M. A. Klochko and M. M. Godneva, J. Inorg. Chem., (U.S.S.R.) 4, 964 (1959)

37. V. G. Levich, "Physicochemical Hydrodynamics," p. 372, Prentice-Hall, Inc. (1962)

38. S. Szpak, C. J. Gabriel, and T. Katan, J. Electrochem. Sec. 127, 1063 (1980).

39. T. Katan and S. J. Szpak, "Basic Studies on Fuel Cell Systems," NOw60-0738-d, Final Report LMSC #2-99-63-3, July 1963.

SECTION 8

FIGURES

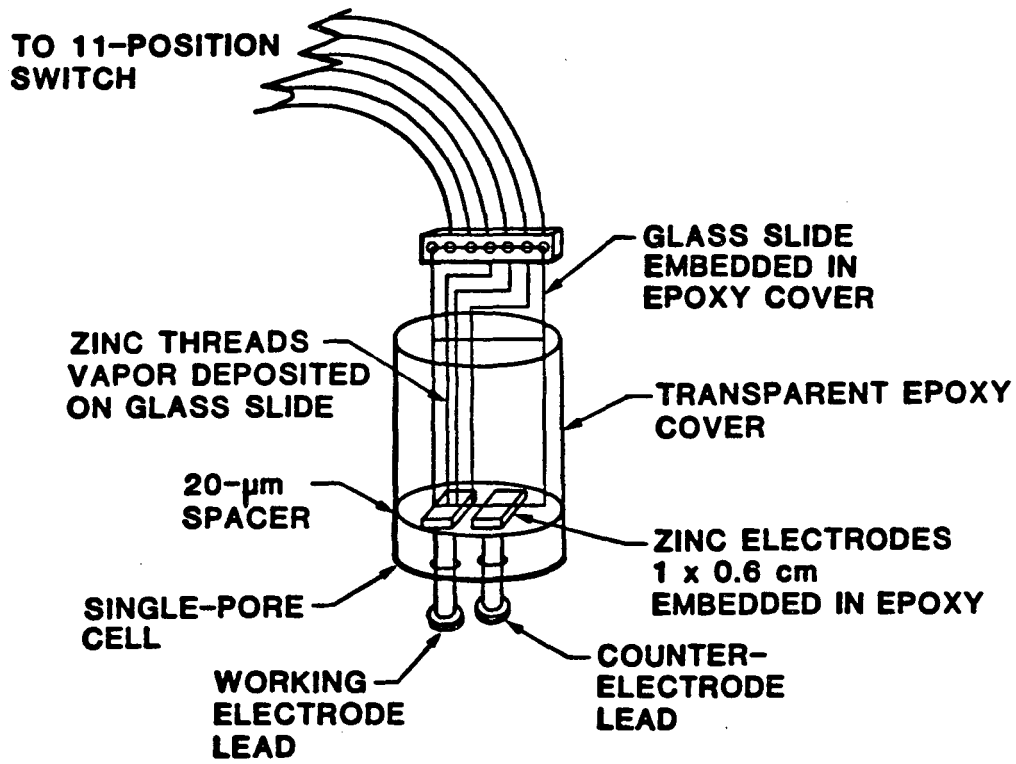

FIG. 1. Schematic diagram of single-pore zinc cell with multiple-reference electrode attachment.

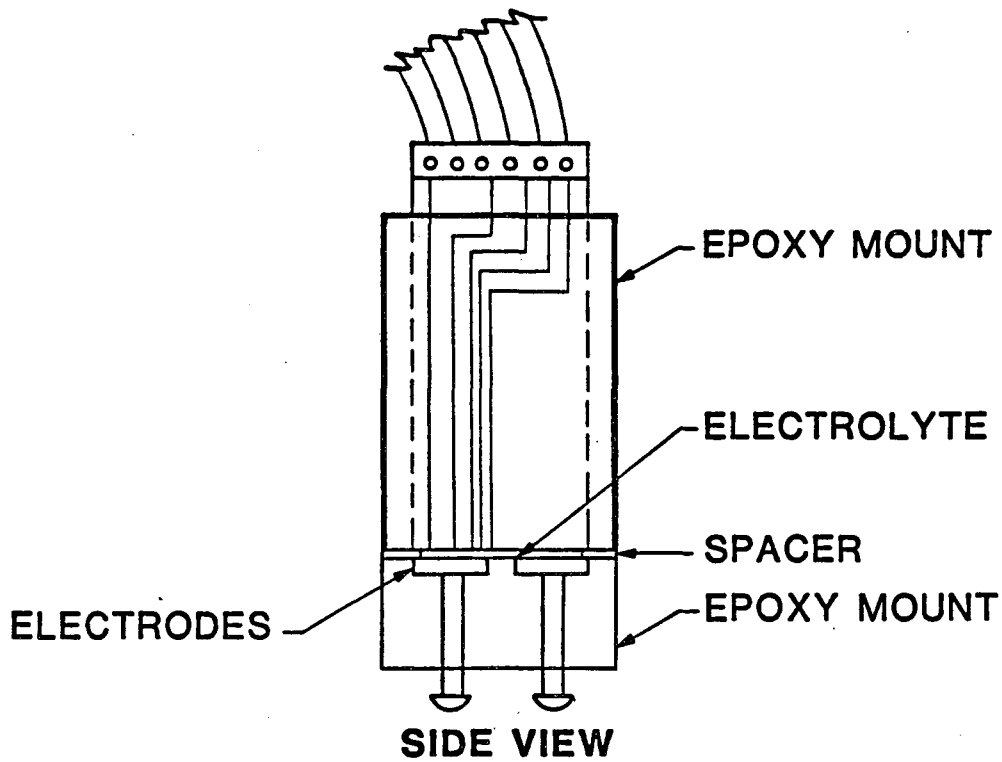

FIG. 2. Schematic diagram showing placement of multiple-reference array with relation to working electrode.

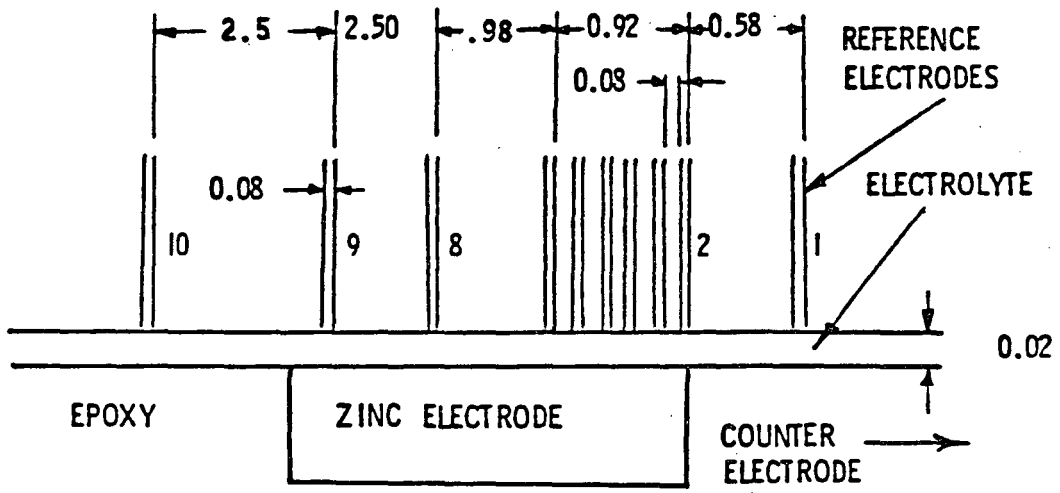

FIG. 3. Details of locations of reference electrodes above working electrode.

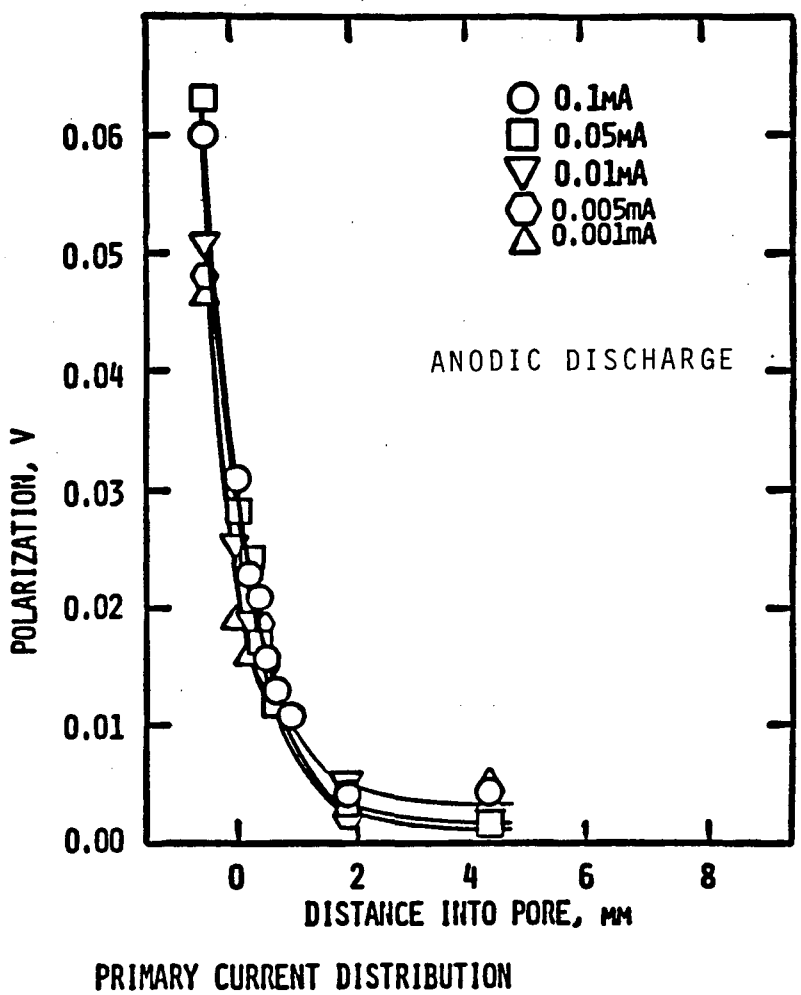

FIG. 4. Secondary polarization distribution within single-pore, 0.005 mA to 0.1 mA. Slotted pore, 1 cm x0.0020 cm, 10 M KOH, Sat'd ZnO, Zn wall.

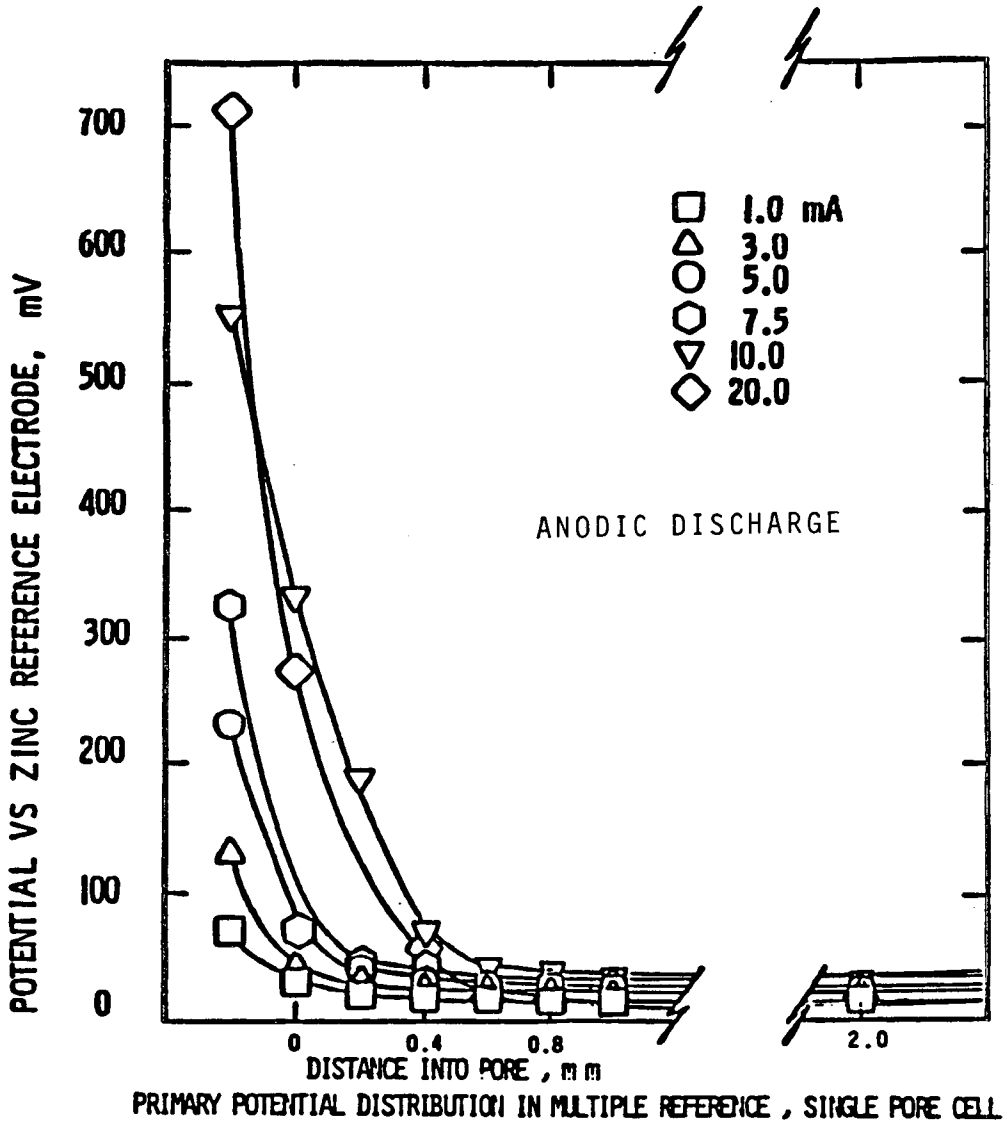

FIG. 5. Secondary polarization distribution within single-pore, 1.0 mA to 20 mA. Slotted pore, 1 cm x 0.00020 cm, 10 M KOH, Sat'd ZnO, Zn wall.

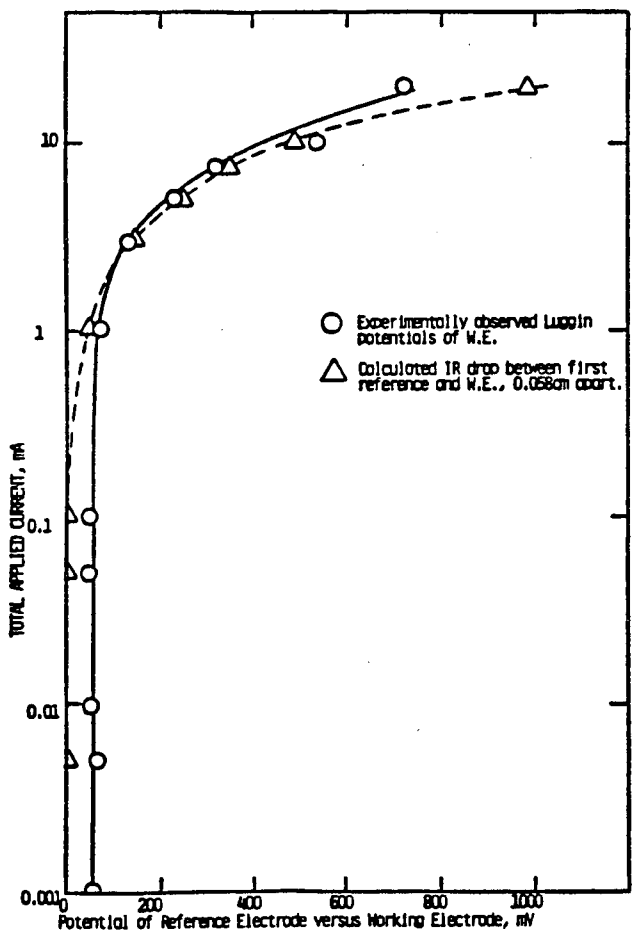

FIG. 6. The initial "Luggin" potential of the working electrode and the calculated IR correction.

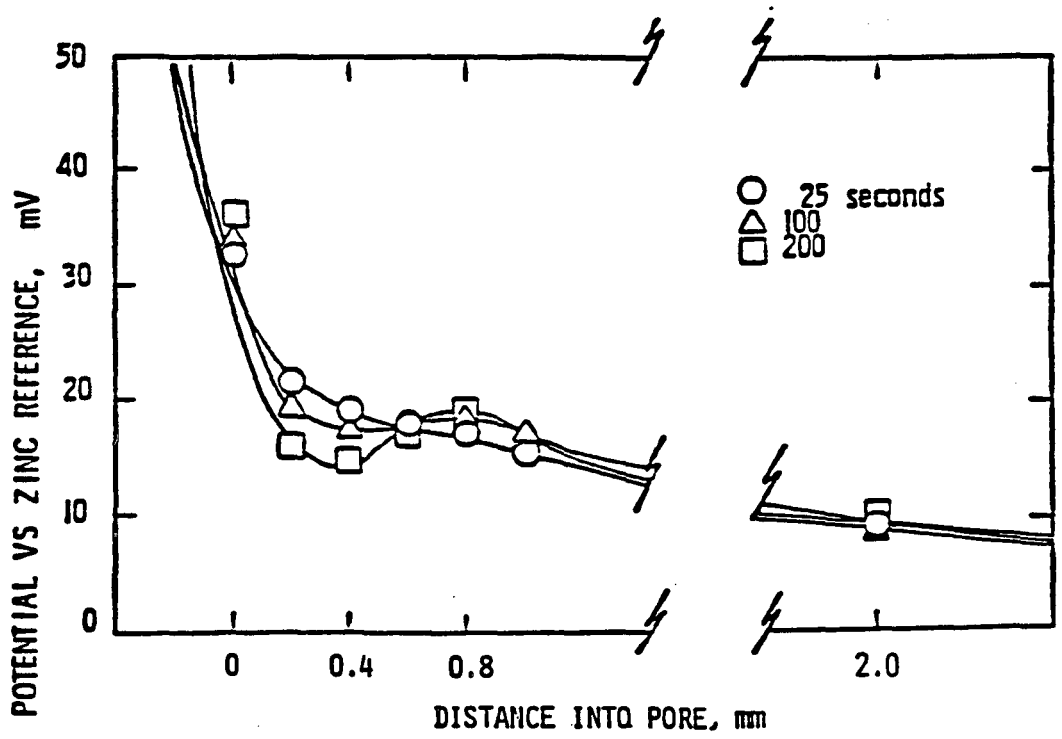

FIG. 7. Evolution of potential profiles in pore electrode, 1 mA applied current.

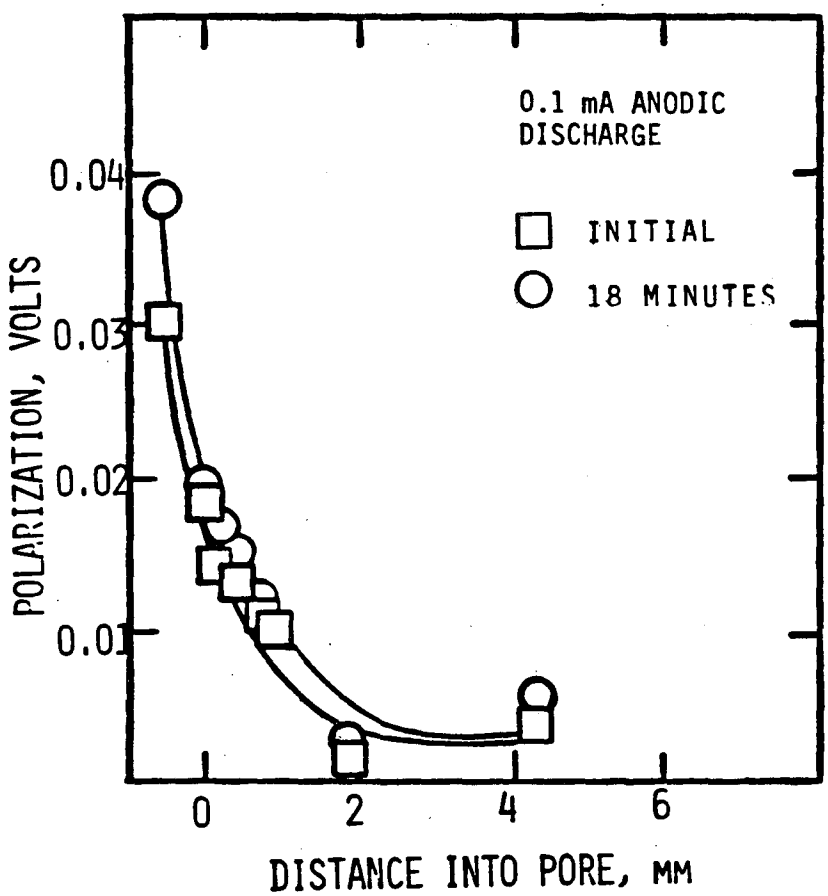

FIG. 8. Potential profile for 0.1 mA applied current.

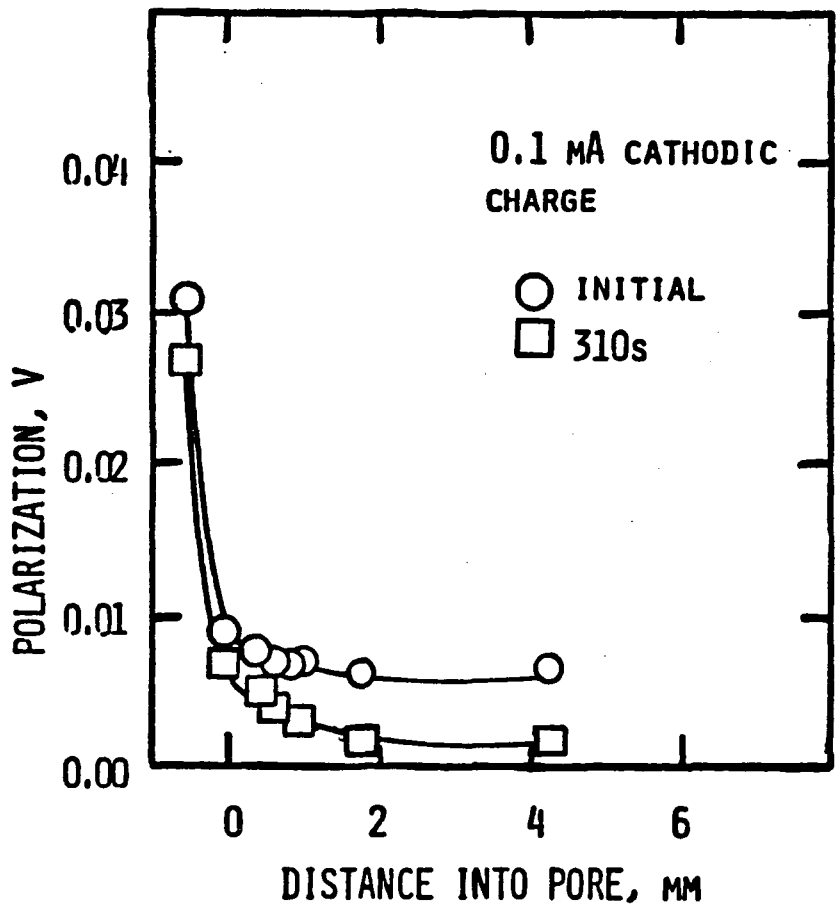

FIG. 9. Cathodic potential profile developed during cycling. Decrease in polarization with time passage results from increasing surface area.

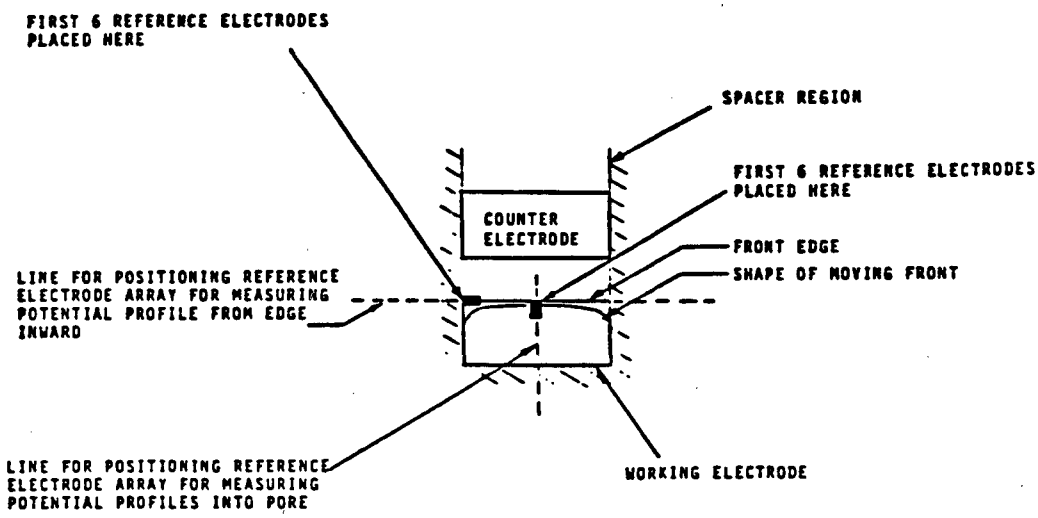

FIG. 10. Schematic diagram showing placement of reference electrode array for measurement of potential profile into the pore and along the front to obtain edge effects.

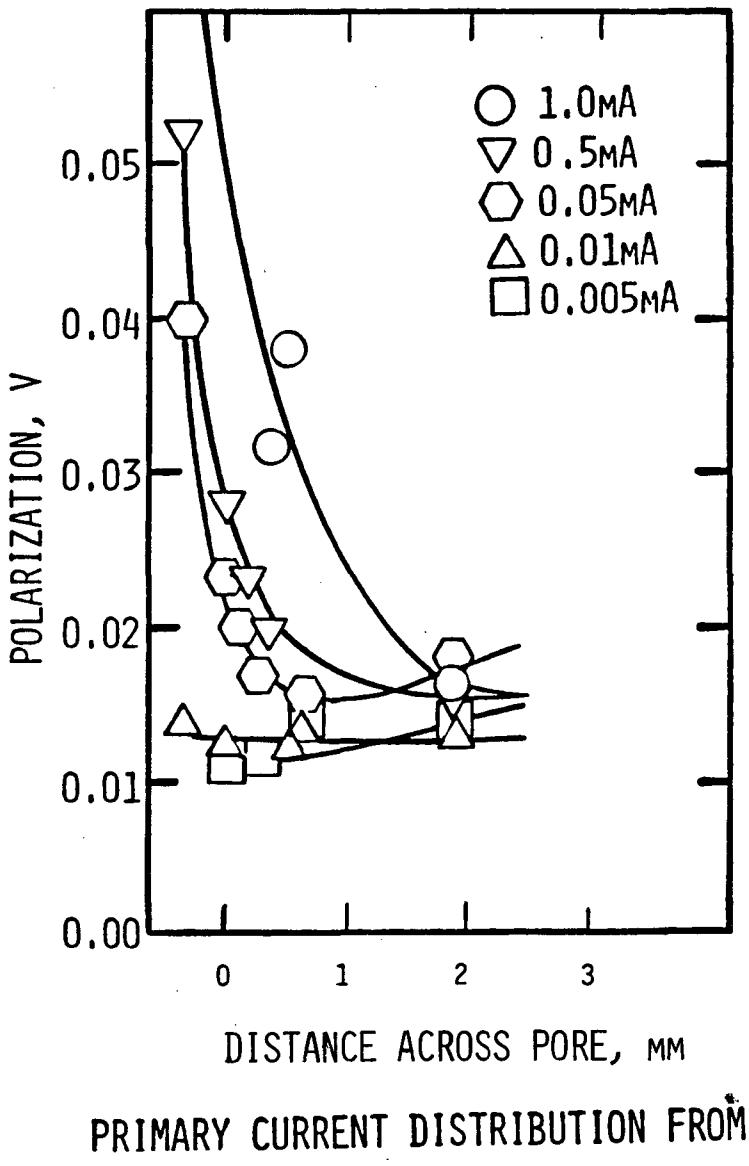

FIG. 11. Edge effect at various currents.

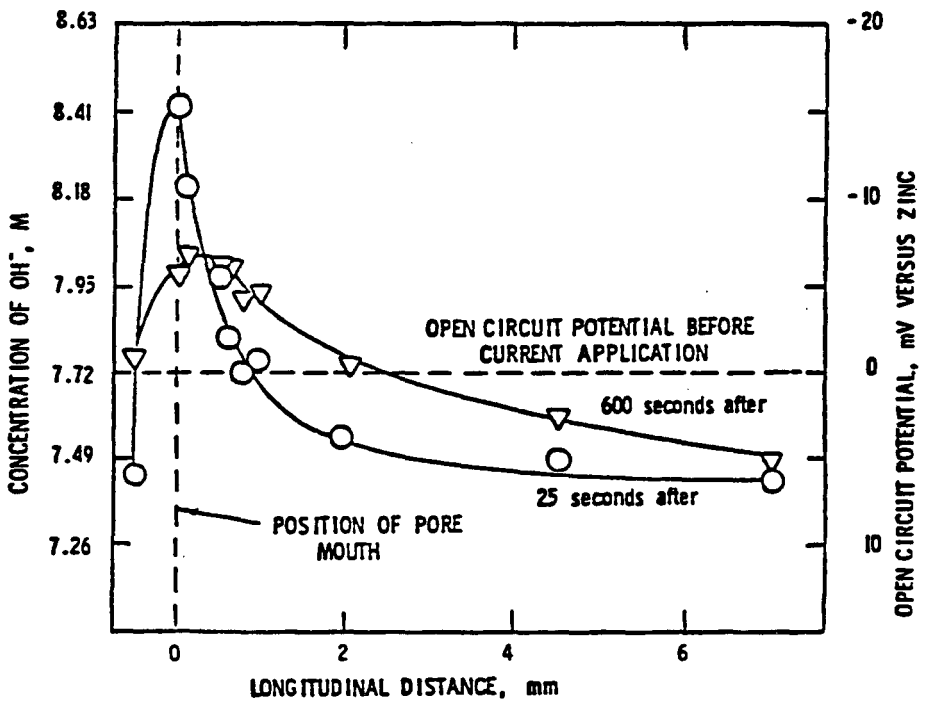

FIG. 12. Concentration and open-circuit potential profiles. Taken 25 and 600 seconds after closed-circuit anodic discharge at 1 mA for 86 seconds.

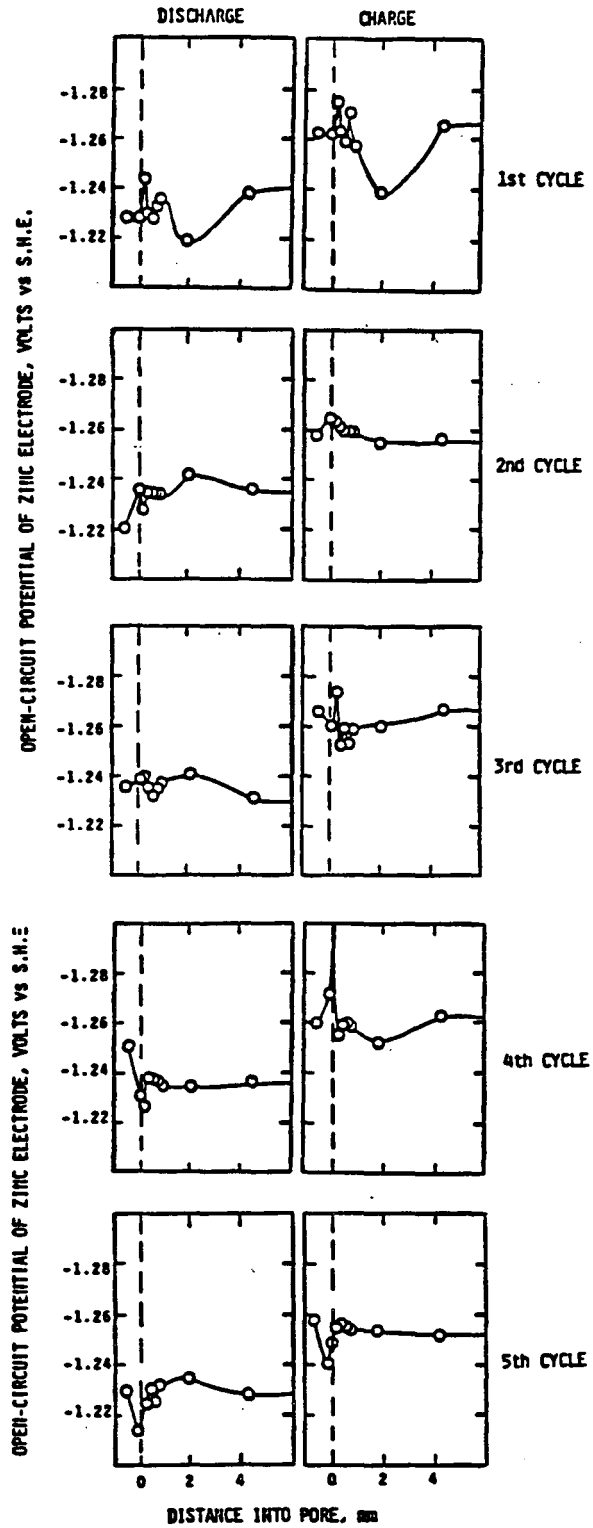

FIG. 13. Open-circuit potential profile after discharge and charge, 120 seconds each, 1 mA.

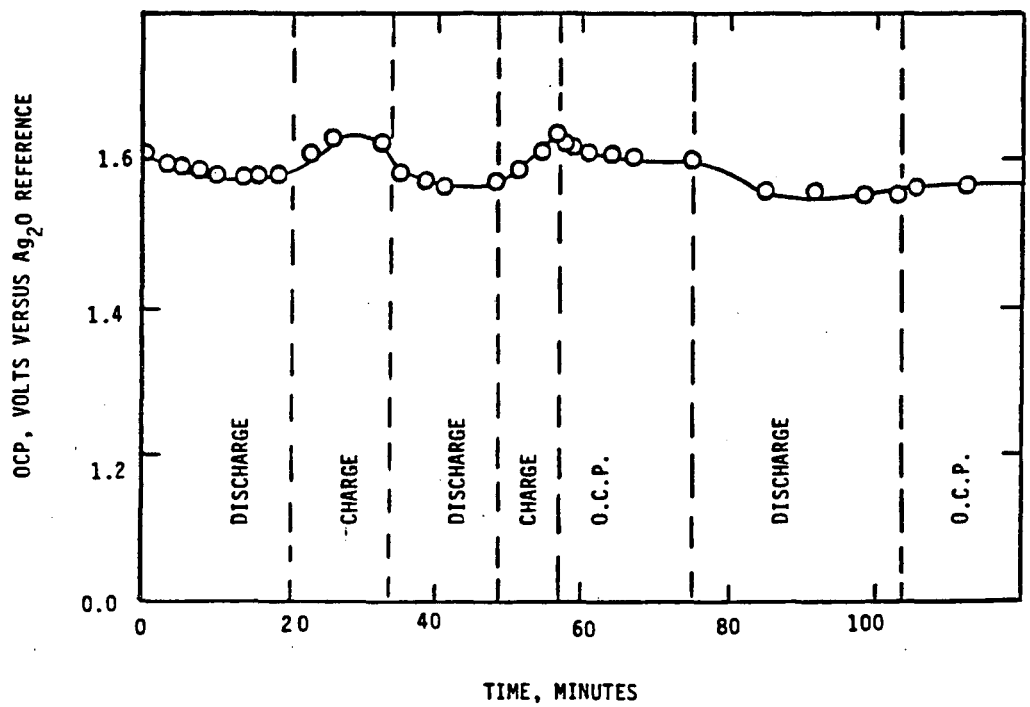

FIG. 14. Overall open-circuit potential, 0.1 mA.

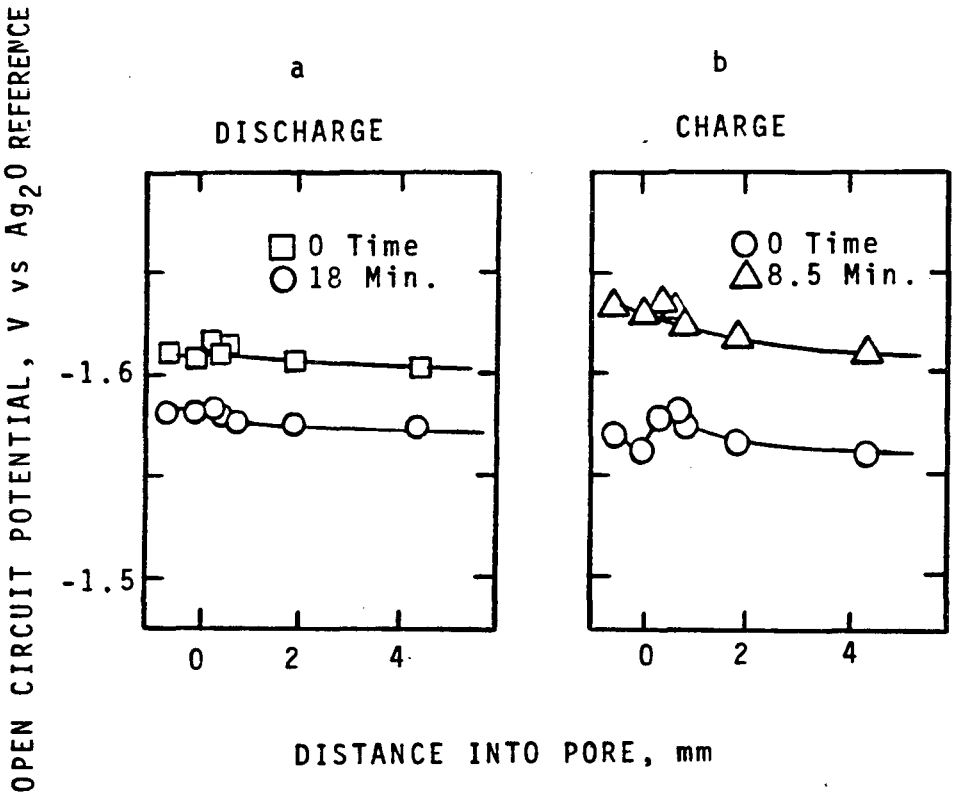

FIG. 15. Open-circuit potential profile, 0.1 mA.

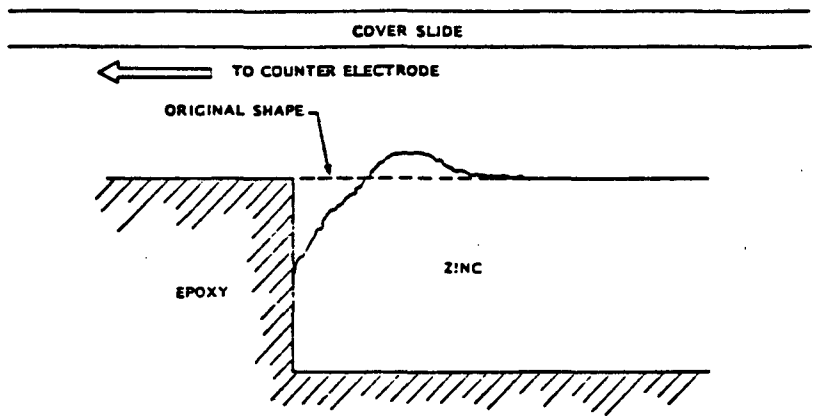

FIG. 16. Zinc movement after cycling single-pore cell.

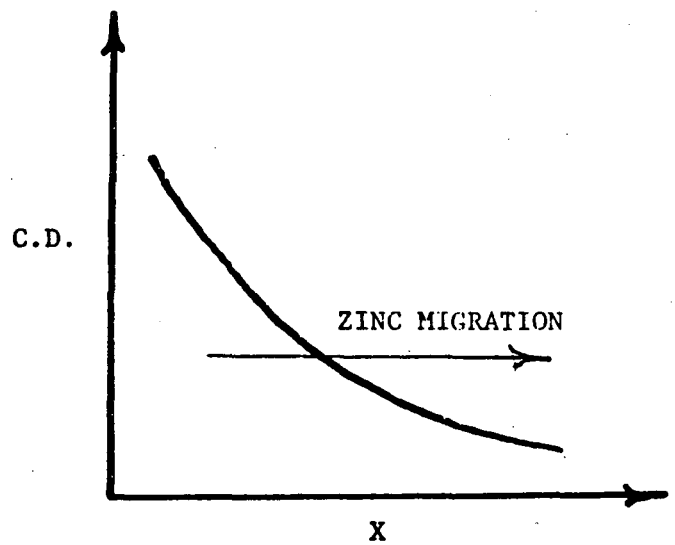

FIG. 17. General direction of zinc metal migration in cycled, closed, and compact electrochemical systems.

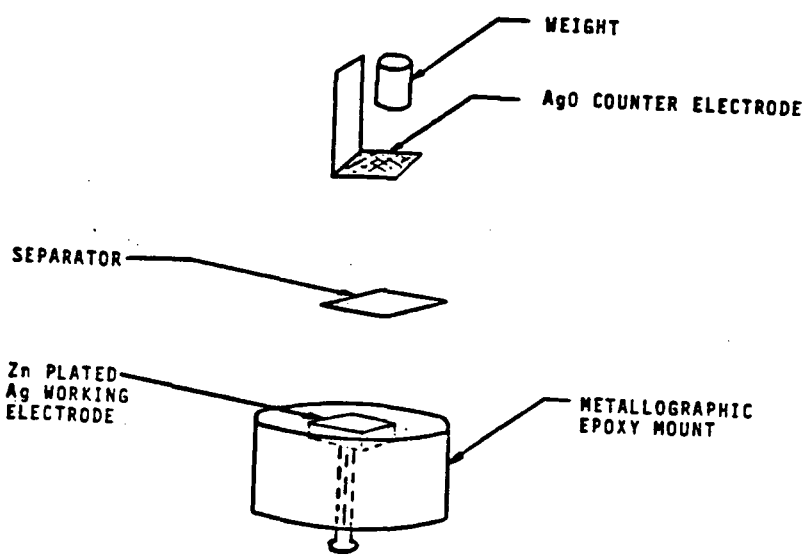

FIG. 18 Schematic diagram of an opened planar electrode cell assembly.

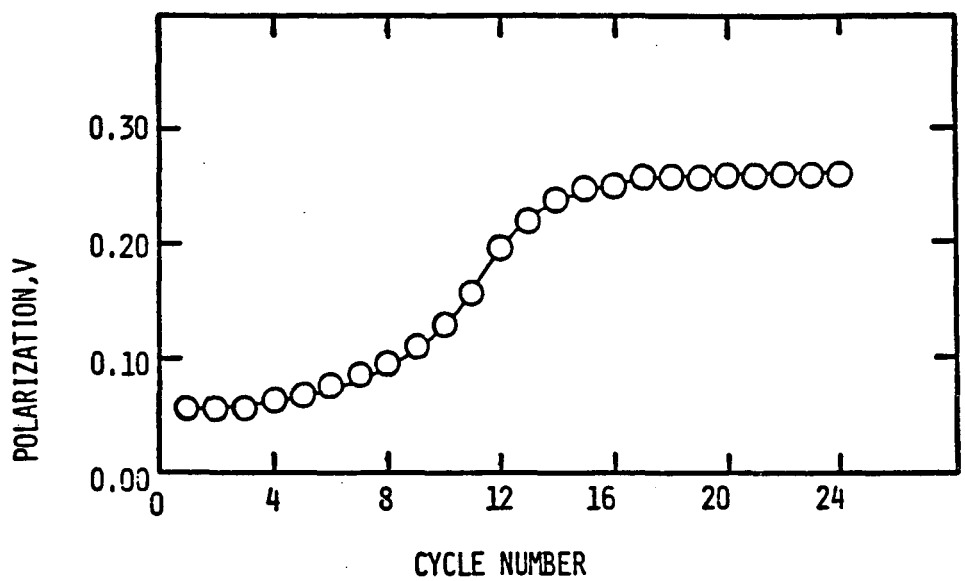

FIG. 19. Gradual improvement in performance when cycling at 100 mA, 10 seconds each way.

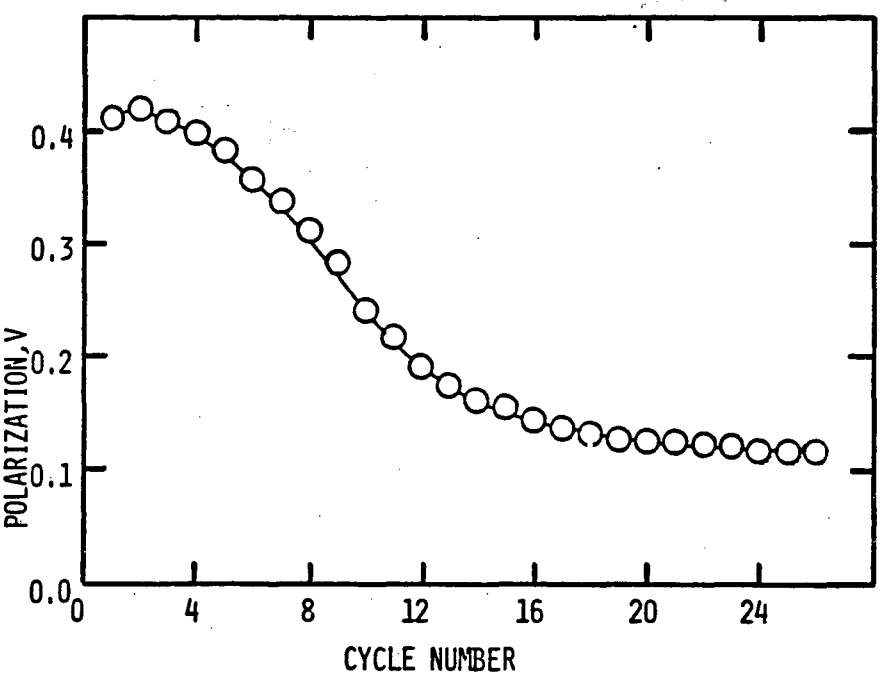

FIG. 20 Gradual decrease in performance when cycling at 35 mA, 30 seconds each way.

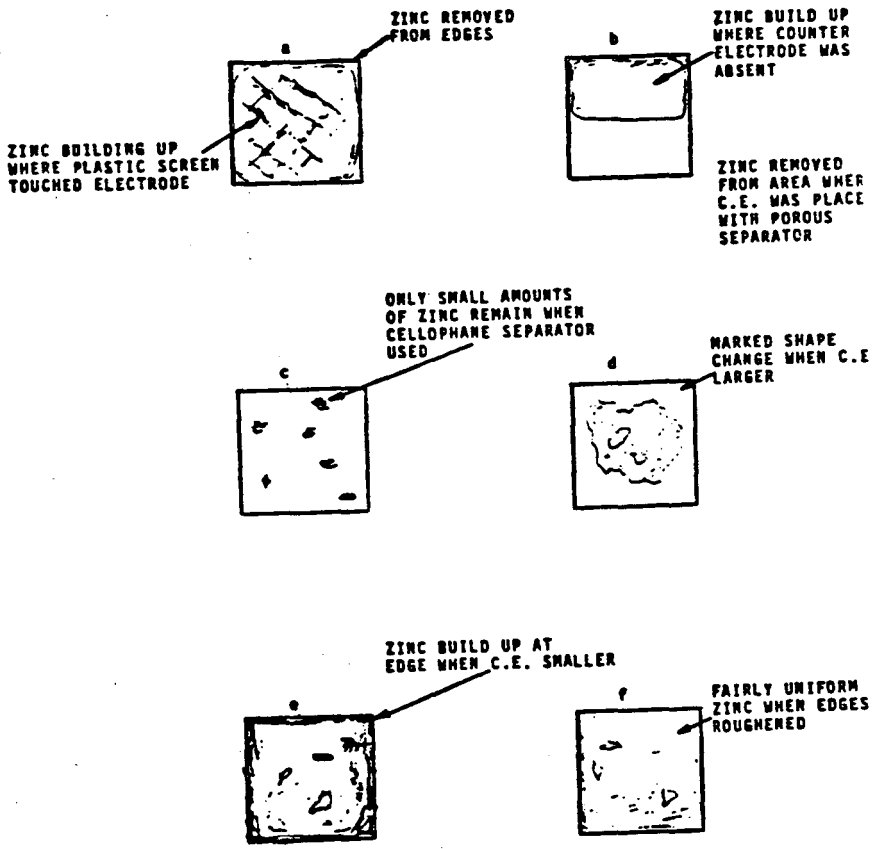

FIG. 21. Various patterns observed on the planar zinc electrode after cycling. a. With an open, 10-mesh polypropylene separator; b. With a displaced counter electrode; c. With regenerated cellulose separator; d. With a larger counter electrode; e. With smaller counter electrode; f. With roughened edges.

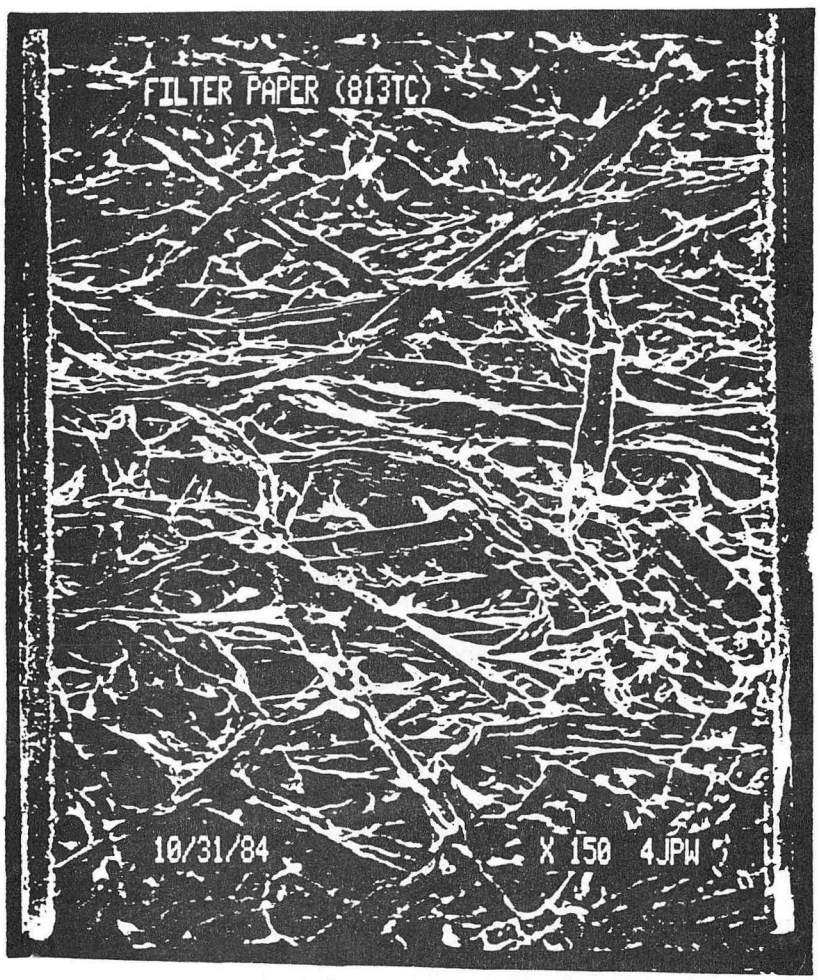

FIG. 22. Separator paper structure.

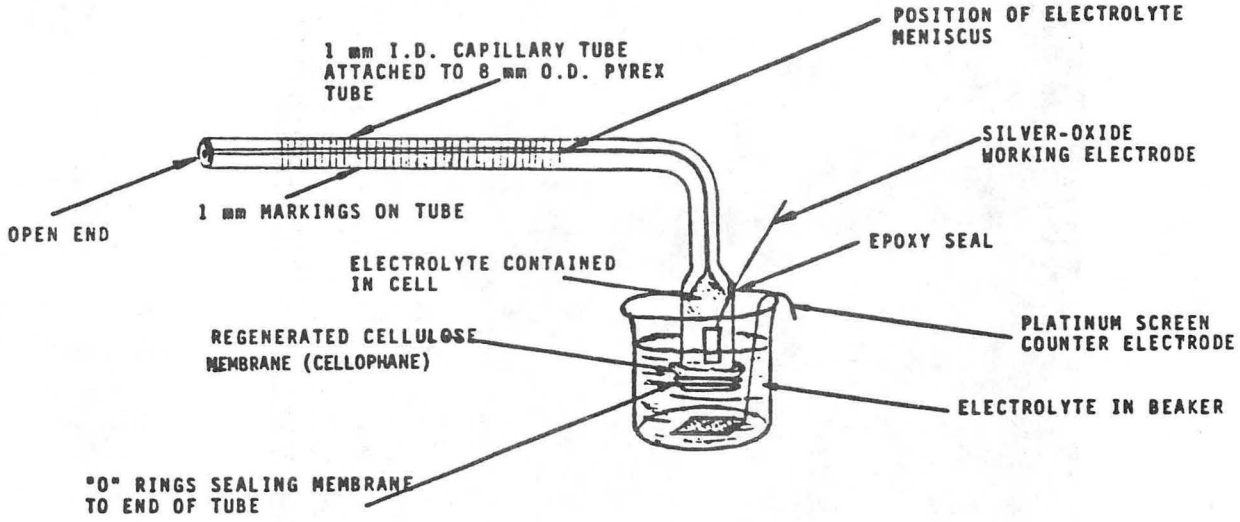

FIG. 23 Cell for Osmotic/Electroosmotic Studies.

This report was done with support from the Department of Energy. Any conclusions or opinions expressed in this report represent solely those of the author(s) and not necessarily those of The Regents of the University of California, the Lawrence Berkeley Laboratory or the Department of Energy.

Reference to a company or product name does not imply approval or recommendation of the product by the University of California or the U.S. Department of Energy to the exclusion of others that may be suitable.

LAWRENCE BERKELEY LABORATORY
TECHNICAL INFORMATION DEPARTMENT
UNIVERSITY OF CALIFORNIA
BERKELEY, CALIFORNIA 94720